IEEE Access
Multidisciplinary | Rapid Review | Open Access Journal

Received January 8, 2021, accepted January 17, 2021, date of publication January 26, 2021, date of current version February 5, 2021.

Digital Object Identifier 10.1109/ACCESS.2021.3054792

Improvements in Existing System Integrity Protection Schemes Under Stressed Conditions by Synchrophasor Technology–Case Studies

MAKARAND SUDHAKAR BALLAL[1], (Senior Member, IEEE), AND AMIT RAMCHANDRA KULKARNI[2], (Student Member, IEEE)
[1]Department of Electrical Engineering, Visvesvaraya National Institute of Technology, Nagpur 440010, India
[2]Maharashtra State Electricity Transmission Company, Mumbai 400051, India

Corresponding author: Amit Ramchandra Kulkarni (amitkul2019@rediffmail.com)

ABSTRACT In this modern era, the power system is stigmatized by a conglomeration of ultra-high voltage AC and DC, multi-terminal DC, and extra-high voltage AC transmission networks. It consists of a large distribution network beyond the country along with traditional generation having Ultra Mega Power Plants (UMPP) and growing ingress of Renewable Energy Sources (RES). The System Integrity and Protection Schemes (SIPS) play a crucial role in preserving a secure and reliable grid and facilitate efficient grid control during severe power system contingencies. In this paper, the operational experiences of three important SIPS in India are presented. Based on a thorough analysis, the drawbacks of these SIPS are identified and an algorithm is proposed to overcome the drawbacks using synchrophasor technology. The performance and capability of the proposed algorithm are evaluated by simulation studies on the 39-bus New England system embedded with HVDC link in MATLAB. Simulation results consummated confirm the effectiveness of the scheme in preserving system integrity. Results are validated using Electrical Transient Analyzer Program (ETAP), which is a very powerful design and analysis tool and has an extremely user-friendly interface.

INDEX TERMS Operational experience, performance evaluation, system integrity and protection schemes (SIPS), power swing, distance relay, MATLAB, ETAP.

I. INTRODUCTION

System integrity protection schemes (SIPS) are special protection schemes that can operate under stressed conditions and prevent blackout of vulnerable parts of an electrical power system. The prime aim of SIPS is to supervise the condition of the power transmission grid in real-time and to react in exigency situations. The accomplishment of the effective performance of SIPS is the challenge before the research community. In literature, various techniques and methods are reported for the design, performance evaluation, and improvements in SIPS [1]–[5]. A joint IEEE-CIGRE survey to clinch the experience with SIPS and to knock the designers and operators of these schemes concerning the reliability of their performance is reported in [6]. It includes the process, and the rational approaches used to alleviate reliability in the design.

The associate editor coordinating the review of this manuscript and approving it for publication was Hazlie Mokhlis.

The online manifestation of feedback, i.e., response-based Wide-Area stability and voltage Control System (WACS) is given in [7]. The control system constitutes phasor measurements at abundant substations uses uneven actions for power system stabilization. An adaptive fault detection technique stands on phasor measurements for the transmission line is explained in [8]. In this, the voltage and current phasors at both ends of the transmission line are accessed through the Phasor Measurement Unit (PMU). The fault location is deceived from the online calculated system's impedance. Article [9] describes protection and control systems based on several synchrophasors. It only includes a synchrophasor application for generator shedding and ground faults protection for the transmission line. Two major disturbances, such as generation loss and change in loads are studied in [10]. The wavelet method is used to attain the attributes of frequency and voltage derivatives for analysis. But, the generalized symmetrical and asymmetrical faults are not investigated thoroughly.

The analytical and computational approach used to determine fault location in a transmission network is studied in [11] which covers online and offline stages. The online stage measures the time of traveling waves promulgating from the fault appearance point. The scrutiny of the SIPS emended with Norwegian power system and its security assessment study are reported in [12]. However, solutions by these SIPS are not in order. A procedure for constructing SIPS that achieves an agreement between dependability and security is given in [13]. It uses fault tree analysis and the theory of minimal cut sets to impart the reliability analysis of the entire SIPS. But the cost of applying the voting scheme which was commonly employed for improving the prediction stability is not considered in this work. The fault location method uses precisely located wide-area synchronized phasor measurements are discussed in [14]. In this, the faulted system is modeled by a comparable bus injections system which delivers the same transform in bus voltages with the fault current corresponding to a fault. Thus it requires an authentic three-phase framework and an abundant number of phasor measurements.

An approach based on integrated protection, described in [15] is used for improving the security of protection operations. Weak links, which may mal-operate during a stressed condition are identified. But, the output of the algorithm is evaluated using synchronized voltage and current phasor data for a limited time frame. A number of the concepts which can assist to resolve several eventful threats to the power system protection are explained in [16]. It includes wide-area disruption, power system blackouts, cascade trippings of protection relays in complex working conditions, etc. However, the proper management of wide-area disturbances is still beyond the scope of most of the existing protection schemes. Thus, adaptive system integrity protection schemes are needed to protect power system security. A PMU-based method for calculating transmission line parameters from PMU data at receiving and sending ends of a line is explained in [17]. The identification accuracy is improved by median estimation instead of PMU phase angle measurement to avoid the errors caused by synchronization problems. The steady-state PMU data that do not contain system disturbances used and transients are not taken into considerations.

In [18], the normalized wavelet energy function is used to calculate the root mean square value of coefficients obtained from time-synchronized voltage and frequency signals. It reflects the non-stationary occurrence of major changes in these signals. The normalized wavelet energy (NWE) values are received by real-world PMU event data did not include symmetrical and asymmetrical faults. Also, the relationship between NWE and event locations has not been elaborated. A measure to estimate mal-operations and undesirable interactions between various SIPS on the same or adjoining systems is studied in [19]. SIPS with adaptive protection philosophy that could adjust to the changing system conditions and the attainment of other protection schemes are also explained. However, the risk introduced by using SIPS with fixed logic varies accordingly with the wind outputs from the wind farms. Therefore, the adaptive SIPS need to be implementing as they offer a noticeable reduction in SIPS risk as well as its variation.

In [20], voltage and current phasors of fundamental frequency components are used for the segregation of power swings and metallic faults. Diagnoses of the important features were carried out by the alternator models in the stability studies. But the delta based algorithm is no faster and another admittance based algorithm is all the time requires. A shutdown of an ultra-mega-power project (UMPP) in western region of India disturbed by the operation of protection relay during power swing is described in [21]. In this, a SIPS is invented to mitigate instability occurred by cause of unstable power swing. The work is restricted to certain defined conditions and changes in power swing are not considered. SIPS explained in [22] determine the relay security index based on apparent impedance to avert mal-operations of protection relays under sprained conditions. Even though the scheme is stable for changes in network topology but it response only for first swing stable exigencies. Also under stressed conditions, mal-operations of protective devices are not examined thoroughly.

The operating characteristics implemented in the modal current ratio plane are shown in [23]. The method is restricted to a twin circuit transmission line. In case of sudden relay setting, the scheme did not respond timely but it acquires some delay. Also, the sensitivity of relay was hampered in CT saturation conditions. In [24], distributed SIPS architecture is demonstrated for enriched resiliency and availability based on synchrophasors technology. However, AC optimal power flow to the SIPS needs to be explored. The SIPS applications are based on few control types and not on any practical incidence. A pilot scheme for the accelerated secured operation of zone-3 under tense system conditions is expressed in [25] on the IEEE 39-bus system. The dedicated communication bandwidth is the mandatory requirement for this scheme. In this, highly accurate co-ordination of the distance element zones is required to accelerate zone-3 operations. Article [26] provides an outline of the structure and utilization of wide-area monitoring, protection, and control (WAMPAC) system. This serves as SIPS to monitor, protect, and control transmission power during normal and abnormal operating conditions. The use of PMU technology for the enhancement of SIPS as a part of WAMPAC systems is described in [27]. In this, the optimal bus splitting scheme pinpoints potential actions that can decimate the power system burden and protect the integrity of the power system. However, the performance of SIPS has not been judged analytically for a generation back down and load-shedding, including under-frequency and under-voltage protection schemes.

Model predictive control based strategy is explained in [28], which repeatedly updates the power set points of the Multi-Terminal DC (MTDC) converter stations and alternators to mitigate AC line overloads. The controller is attached

to the classical automatic generation control. This controller mandatorily needs to checks a voltage stability criterion to ensure that it does not push the system towards the voltage instability boundaries. Support by synchrophasor measurement to SIPS for the exclusive high-end protection of the smart power grid is given in [29]. It extricates synchronized voltage and current phasor data from all phasor measurement units. It is used to identify the disturbance, detect the disturbed area, and locates the responsive region and thus improves the situation awareness. In this SIPS, the appropriate actions such as generation or load adjustment or controlling under voltage or over voltage relay operation are not demonstrated. A cyber-attack resilient protection scheme based on a multi-agent system is explained in [30]. In this, a state-aware protocol is promoted to facilitate data exchange among agents. Thus, the decentralized protection scheme has flexibleness when facing malevolent attacks compared to ordinary centralized protection. A comprehensive analysis of the timing performance of the algorithms needs to be carefully examined for specific requirements.

In [31] attempt is made for the detection of a specific type of faults on the transmission line, using phaselets computed from PMUs. However, it did not predict the location of the fault accurately on the transmission line and thus there is no scope for situational awareness. In [32] the adequate and economic performance class of PMUs are determined that can meet the proper performance of the distribution system state estimation (DSSE). It is judged using numerical experiments on a distribution system characterized by an unbalanced operation and an asymmetric structure. However, the distribution system operator needs to select proper performance criteria in light of operational applications that use the distribution system state estimation results. A technique for determining the reporting latency of a PMU is demonstrated in [33]. However, using the simulation phasor data directly for protection or other real-time applications is very unrealistic because it does not incorporate the latency associated with the measurement window of the PMU.

This paper presents the operational evaluation of three existing SIPS in the western and northern regions of India. The major contribution of this research paper is mentioned below.

i. New England IEEE 39-bus system is designed and embedded with HVDC link in commercial available programming language MATLAB and performances of all three SIPS are tested.
ii. Discrepancies of the existing SIPS are determined.
iii. Algorithm is proposed for the removal of these discrepancies.
iv. Performances of existing SIPS in coordination with the proposed algorithm were analyzed.
v. The results of MATLAB simulations are validated by comparing them with the results from ETAP.
vi. The constructive analysis based on information across a wide area is carried out. Ingenious control actions are coordinated through a proposed algorithm.

The proposed algorithm when incorporated with the existing SIPS delivers many advantages. It is adaptive for any SIPS and its operation is based on only PMU data. There is no need for any historical data or prediction and or estimation methodology. PMU measurement endows the SIPS to avoid burdensome power network modeling, thus drains the potential errors. Satisfactory performance is demonstrated as the accuracy of operation is more than 95% and achieves closed-loop control with robustness. Augmentation due to the proposed algorithm can tackle normal as well as abnormal or fault conditions in real-time, including unforeseen events. Convenient control actions can be accredited without negotiating to the high speed of response.

The rest of the paper is organized as follows. The operational evaluations of three existing SIPS in India are elaborated in Section 2. The proposed methodology is given in Section 3 to overcome the drawbacks in existing SIPS. In Section 4, the effectiveness of the proposed scheme is demonstrated from the assorted simulation results obtained from a modified IEEE 39-bus system embedded with DC link in MATLAB. Validation is done by comparing it with the results obtained from the Electrical Transient Analyzer Program (ETAP). Concluding remarks are given at the end in Section 5.

II. MOTIVATION

India is one of the biggest producers and consumers of electric power in the world. The Indian power systems in respect of planning and operational purpose are segregated into five regional grids. The assimilation of regional grids, and thereby formation of National Grid, gestated in the early nineties. The amalgamation of provincial grids which commenced with asynchronous HVDC back-to-back inter-regional connection facilitating a defined transaction of regulated power was consequently graduated to high capacity synchronous attachment among the regions. As of December 2020, the overview of the Indian power grid is tabulated in Table 1.

TABLE 1. Overview of the Indian power grid [34].

SN	Particulars	Quantity
1	Installed Generation Capacity	378 GW
2	Transmission above 220kV	381671 ckm
3	Transformation capacity above 220kV	791570 MVA
4	Installed Renewable Energy Capacity	65 GW
5	HVDC Bipolar/ Back-to-Back systems	11 Nos.
6	Multi-Terminal HVDC	1
7	Operational SIPS	52

There are fifty-two SIPS are operating in India. They are meant for defined tasks such as tripping of critical lines/ corridors, safe evacuation of generation, overloading of

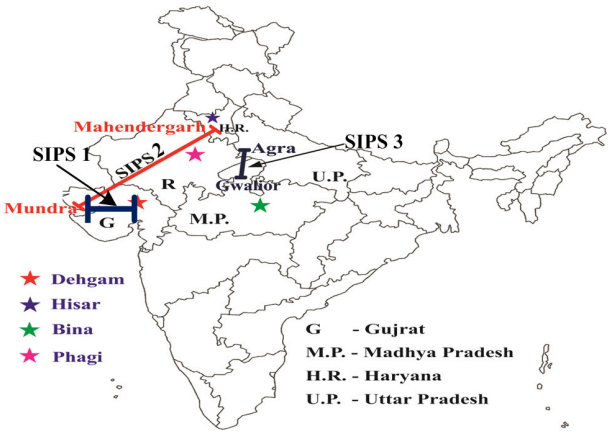

FIGURE 1. SIPS under consideration.

transformers, generation backing down, etc. Three major occurrences in the Indian power system motivate the authors to present this article. Fig.1 shows the representation of SIPS under discussion in this paper and considered for their performance evaluation with their representation on the map of India. The performance evaluation of the three SIPS is discussed in the following sub-sections.

A. BLACKOUT AT CGPL–UMPP INDIA ON 13 JULY 2016

At Mundra, a town of Kutch district in the Indian state of Gujarat, Coastal Gujarat Power Limited (CGPL), operates, control, and maintains 5 units each of 800 MW, thus the total is 4000 MW called as Ultra Mega Power Plant (UMPP). It supplies power to three states in western India viz. Rajasthan, Gujarat, and Maharashtra and two states in northern India viz. Punjab and Haryana. On July 13, 2016, an unstable power swing event causes a complete power failure at CGPL [35]. Fig. 2 depicts the single line diagram of this event with disturbances in 400 kV substations.

SIPS-1 is devised to tackle under system contingency is shown in Table 2. The power of 2875 MW was produced by CGPL before the event. During the occurrence, two subsequent bus faults on 400 kV bus 1 and bus 2 of 400 kV Varsana substation aggravate these events. Earlier, a bus fault took place at 20:29 Hrs. and the components connected to bus 1 got disconnected and a consequent bus fault on bus 2 at 21:50 Hrs. caused the desolation of 400 kV Varsana substation. On charging Bhachau-Varsana-1 line from the Bhachau end, a zone-2 line fault was noticed at Bhachua, CGPL, and at Ranchdopura end.

From the disturbance records, at the time of the incident, the CGPL units were feeding power at the Varsana substation. After charging of Bhachua–Varsana line-1, at 350 ms there were trippings of 400 kV lines with an unceasing downturn of voltage for 290 ms. A rise in voltage was examined eventually at CGPL end as a power swing impinges in zone-1of all the lines. Thus, the distance relays of these lines issue trip signals to respective circuit breakers. These trippings result

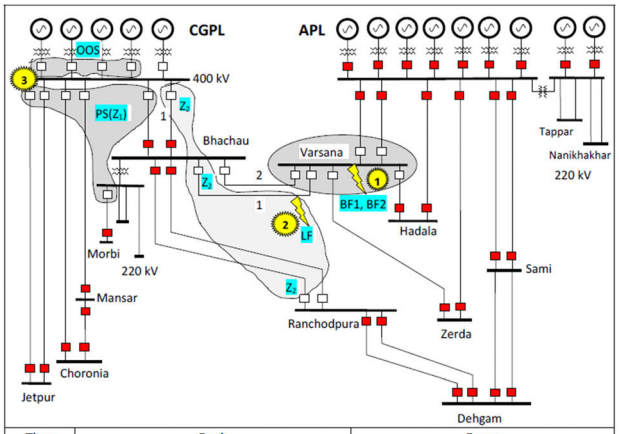

Time	Fault	Event
20:29 hrs	Bus fault (BF1) at 400 kV Bus-1 of Varsana 440 kV Substation	Elements connected to 400 kV Bus-1 & 2 got disconnected.
21:50 hrs	Bus fault (BF2) at 400 kV Bus-2 of Varsana 440 kV Substation	
02:37 hrs	Bhachau-Versona-1 line charged from Bhachau end	Line fault (LF) sensed by Distance Relay in Zone-2 at Bhachua end of the line and further at 1. Ranchdopura end of Bhachau-Ranchodpura lines 2. CGPL end of CGPL-Bhachau-1 line; the lines tripped.
02:37 hrs	Subsequently, power swing (PS) in Zone-1 sensed by Distance relays of remaining five lines at CGPL end.	All five lines tripped. At the same time, Generating units at CGPL tripped on Out of Step (OOS)

FIGURE 2. SLD with a history of occurrence at CGPL [35].

TABLE 2. Existing SIPS-1 [35].

Triggering Event	Action Plan
If exports exceed 3100 MW and any one of the lines trip or if line loading of any line exceeds 900 MW	Reduce the generation of two units to 800 MW
If exports exceed 3100 MW and if CGPL-Bachhau double circuit line trips	Trip one unit immediately
If CGPL-Bachhau double circuit line trips, CGPL-Jetpur or combination of one circuit of each of Bachhau or Chorania or Jetpur trips	Reduce generation to 800 MW such that the loadings of rest of the lines are below 900 MW

in unstable power swing as the oscillations were not damped. Subsequently, Out of Step (OOS) protection was activated for alternators at CGPL. This leads to a generation loss of 2875 MW. Fig. 3(a) illustrates the pre-fault and post-fault voltage and current.

It is seen that a 237–95 kV contraction in the phase voltage during the fault. It is also observed that, as soon as the 400 kV CGPL-Bhachau-1 and 400 kV Bhachau-Ranchodpura twin circuits have opened the voltage enhanced to 108 kV at CGPL. Thereafter, even though the fault got cleared, the voltage collapses. Consecutively, even after the removal of a faulty section from the system, the voltage abstained continuously.

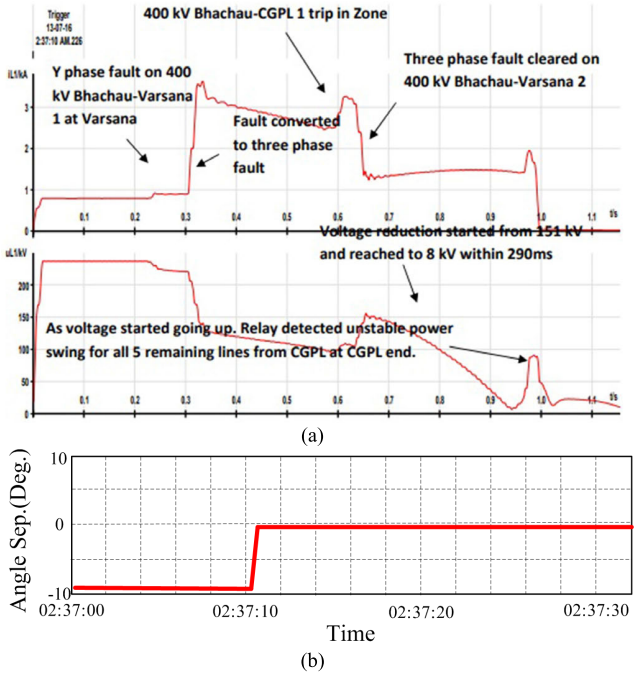

FIGURE 3. 400 kV CGPL-Bhachau Line 2 (a) Voltage and current, and (b) Angular Separation at CGPL [35].

TABLE 3. Existing SIPS-2 [35].

Triggering Event	Action Plan
Blocking one pole and decrement in power submission at Mahendergarh between 600 MW - 900 MW	Load Shedding 300 MW in NR: Haryana (150MW), Punjab (50MW), Rajasthan (50 MW), and Uttar Pradesh (50 MW). Trip generating unit 1 at CGPL, Mundra Power Plant
Blocking one or both pole and decrement in power submission at Mahendergarh between 900 MW - 1250 MW	Load Shedding 600 MW in NR: Haryana (300MW) along with Punjab, Rajasthan, and Uttar Pradesh 100 MW each. Trip generating unit 1 and back down generating unit 2 at CGPL, Mundra Power Plant
Blocking both poles and decrement in power submission at Mahendergarh between 1250 MW - 2000 MW	Load Shedding1400 MW in NR: Haryana (600 MW) along with Punjab, Rajasthan, Uttar Pradesh, and Delhi 200 MW each. Trip generating unit 1 and 2 and back down generating unit 3 at CGPL, Mundra Power Plant

Power swing was perceived in all the five lines originating from CGPL. Fig. 3(b) shows angular separation at the time of the incident. The observation regarding transient stability studies done by an expert study group is available in [35]. The following suggestions are given by this study group. (i) Line differential protection shall be employ as critical fault clearance time for the complete network was 100 ms. (ii) Power swing upsetting distance relay operation on instances of fault is quite more. (iii)Simulation studies in the event of unstable power swing demonstrate that tripping of one of the CGPL units mitigates the oscillations after the clearance of fault by 300 ms. (iv) Existing special protection scheme needs to be modified. After the 2012 Indian blackout, the task force had advocated tripping the line and block tripping of all other zones during power swing except zone-1.

B. TRIPPING OF ± 500 kV HVDC LINE ON 8, JAN. 2016

India's first HVDC bipolar 2500 MW, 500 kV, 960 km line shown in Fig. 1 is in private hands. This link traverses between the Mundra in the western region (WR) to industrial load centers Mohindergarh in the northern region (NR). The SIPS is devised to deal with a contingency for this HVDC system shown in Table 3. It performs two actions one for generation backing down at Mundra (WR). Another action covers load shedding of selected loads in NR.

This bipolar HVDC link tripped on 8th, January 2016 at 6:40 Hrs. Before tripping, the power flow on each pole was 900 MW and the power import at Mohindergarh was 1800 MW. The variation in power is shown in Fig.4 (a). The system frequency observed at Mundra fluctuates from 49.73 Hz to 49.98 Hz shown in Fig. 4(b). The rise in frequency from 49.85 Hz to 49.95 Hz indicates net load loss during this event. Voltage variations continue for 10 seconds. Due to the sudden loss of load in NR, the angular separation between Dehgam in WR and NR decreased about 10^{o} as indicated by the PMU plot in Fig.4(c). Due to the loss of the HVDC link, the power flow on adjacent 765kV lines is increased. The SIPS devised for the HVDC link came into action for safe and reliable operation of the grid during this incidence. From the existing SIPS architecture, if there is a loss of bipolar link, there will be tripping of two generating units and backing down of the third unit at Mundra. In addition to this, 1400 MW load-shedding imposed in NR shown in Fig. 4(d). For this event, correct SIPS-2 action was observed in WR and NR.

C. TRIPPING OF 765 kV DOUBLE CIRCUIT LINE BETWEEN WR AND NR ON 14 JAN. 2016

765 kV Agra-Gwalior circuit had been conceived as a part of the superpower highway. It was commissioned on 31st March 2007 and provided a synchronous inter-regional link at 400 kV between the NR and WR Grid. The availability of PMU at 400/765 kV sub-stations/power stations along with a robust fiber optic communication network will expedite situational awareness, regulation, and control of power flow to sustain grid parameters. SIPS-3 is devised at

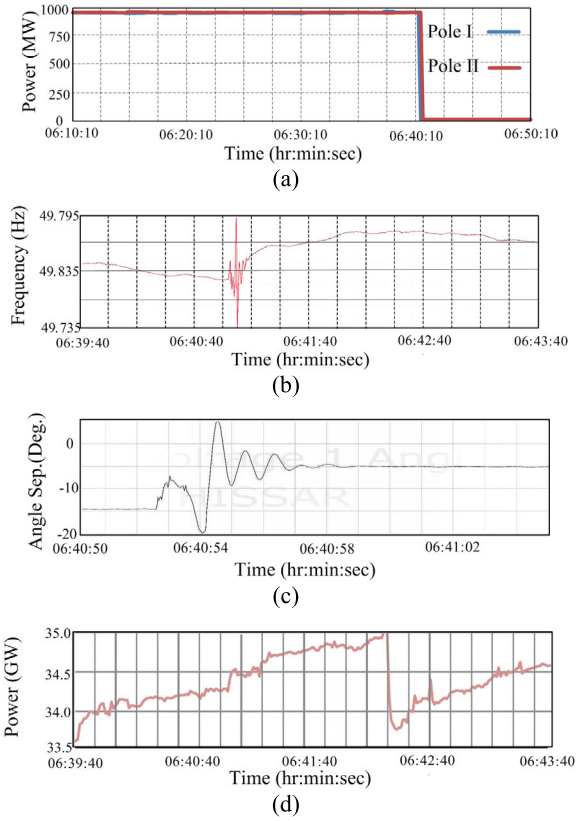

FIGURE 4. Operation of SIPS-2 (a) Power flow variation due to HVDC pole tripping, (b)Frequency variation at CGPL- Mundra PMU, (c) Angular separation, and (d) Load shedding in NR [35].

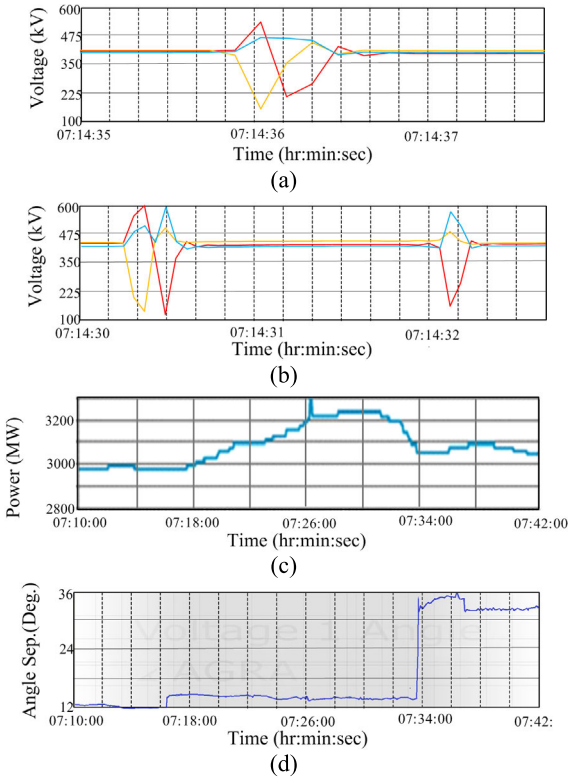

FIGURE 5. Operations of SIPS-3 Voltage dip after tripping of 765kV Gwalior-Agra (a) Circuit 1, (b) Circuit 2, (c) generation back down at CGPL-Mundra, and (d) angular separation observed by Agra PMU.

TABLE 4. Existing SIPS-3 [35].

Triggering Event	Action Plan
If import by NR is between 1000-1500 MW on 765kV Agra-Gwalior Circuit 1and 2	Reduce the generation of two units to 520 MW
If import by NR is more than 1500 MW on 765kV Agra-Gwalior Circuit 1and 2.	Load Shedding 1145 MW in NR

Gwalior (WR) for corrective actions in the event of harsh contingency to prevent grid disturbances is given in Table 4.

On the early morning of 14th Jan 2016, there was dense fog in northern parts of India and various 400 kV lines were under outages. HVDC link Mundra – Mohindergarh was operating in reduced voltage mode with flow restrained to 1000 MW. At 07:14 Hrs, 765 kV Gwalior - Agra Circuit-2 tripped due to earth fault on phase-*a* as indicated by Agra end PMU. Voltage dipped to 155 kV momentarily from an initial value of 430 kV. Tripping of this line has increased the power flow on 765 kV Gwalior-Agra Circuit-1 to 2300 MW. At 07:34 Hrs, 765 kV Gwalior-Agra Circuit-1 also tripped due to earth fault on the phase-*a*.

The maximum voltage dip was observed in the phase-*a* as shown by 400 kV Agra end PMU. Due to the tripping, there was a rise in angular separation from 17 degrees to 34 degrees between Bina (WR) and Agra (NR) substations. Subsequently, SIPS came into operation and there was load shedding of 1200 MW in the states of Punjab, Haryana, UP, and Rajasthan of NR. Generation backing down occurs in WR at Mundra by 180 MW, Korba Thermal Power Station (KTPS) Unit-7 by 145 MW, and Vindhyachal Stage 3 by 250 MW as accomplished in SIPS-3. The complete operation of SIPS-3 under this contingency is depicted in Fig. 5.

From the above investigation, it is observed that power swing was observed in all three occurrences. SIPS did not perform correctly in the first occurrence where the blackout took place at CGPL Mundra. It is because the power swing enters into zone-1, and the protection at Varsana end did not operate correctly. In the next two occurrences, the SIPS operations are found in order. But, this causes excessive load shedding and unwanted back down of generating units. The following section proposes a methodology to overcome these discrepancies.

III. PROPOSED METHODOLOGY FOR THE IMPROVEMENT IN EXISTING SIPS PERFORMANCE

The unwanted trip of transmission lines due to power swings, excessive load shedding, and back down of generating units

are the major problems discussed in the above sections. This section proposes a methodology to resolve these problems by making use of synchrophasor technology. PMU is a device that is used to estimate the amplitude and phase angle of voltage or current on the power grid, using a common time source for synchronization. The cost and other associated restrictions prevent most of the utilities to deploy PMUs at all the buses of the network. Therefore, the optimal location for the placement of PMUs may be decided considering various aspects such as network observability, vulnerability, transient stability, and voltage stability. Network observability based approach may either utilize numerical observability or topological observability. However, in this study, we have not considered any economical constraint and thus PMUs are placed at all the buses.

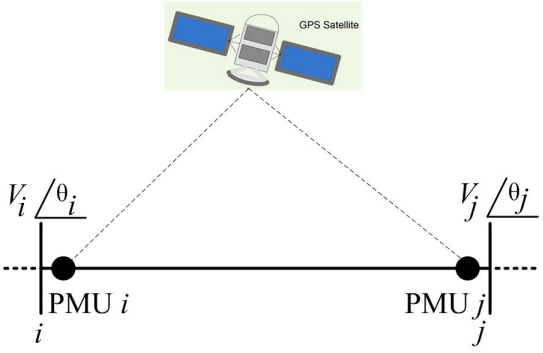

FIGURE 6. Application of PMU for the measurements.

The section of the power grid is shown in Fig. 6 where PMUs are installed at both ends (i and j). This gives RMS values of the voltages (V_i and V_j) and currents (I_i and I_j) and their respective phase angles (θ_i and θ_j). The differential voltage and current are calculated as

$$\Delta \boldsymbol{V}_{\boldsymbol{ij-abc}} = \boldsymbol{V}_{\boldsymbol{i-abc}} - \boldsymbol{V}_{\boldsymbol{j-abc}} \quad (1)$$

$$\Delta \boldsymbol{I}_{\boldsymbol{ij-abc}} = \boldsymbol{I}_{\boldsymbol{i-abc}} - \boldsymbol{I}_{\boldsymbol{j-abc}} \quad (2)$$

During only a power swing ΔI_{ij-a}, ΔI_{ij-b} and ΔI_{ij-c} are zero.

$$\Delta \boldsymbol{I}_{\boldsymbol{ij-a}} = \Delta \boldsymbol{I}_{\boldsymbol{ij-b}} = \Delta \boldsymbol{I}_{\boldsymbol{ij-c}} = 0 \quad (3)$$

During a power swing and a phase-a to ground fault, ΔI_{ij-b} and ΔI_{ij-c} will be equal and zero. However, the ΔI_{ij-a} is not equal to zero. This difference may be used to select the faulty phase. The change in impedance seen by the relay at the end i is expressed as

$$\Delta Z_{ij-abc} = \frac{\Delta \boldsymbol{V}_{\boldsymbol{ij-abc}}}{\boldsymbol{I}_{\boldsymbol{i-abc}}} \quad (4)$$

Only during a power swing, the rate of change of impedance Z_{ij-abc} is zero for the defined time period T.

$$\Delta Z_{ij-a} = \Delta Z_{ij-b} = \Delta Z_{ij-c} = 0 \quad (5)$$

Phase angle discrepancies from PMU are entrenched as an important quantity for immediate monitoring, after any forced outage incident. The present work utilizes the angular dissociation of voltage phasors from PMUs as an early indicator of system stability, strength, and stress. The angular separation between ends (i and j) is given as

$$\delta_{ij-abc} = \theta_{i-abc} - \theta_{j-abc} \quad (6)$$

During only a power swing δ_{ij-a}, δ_{ij-b} and δ_{ij-c} are equal.

$$\delta_{ij-a} = \delta_{ij-b} = \delta_{ij-c} \quad (7)$$

During power swing, if phase to ground fault occurs on phase-a, then δ_{ij-b} and δ_{ij-c} will be equal. However, the angle δ_{ij-a} is less than δ_{ij-b} and δ_{ij-c}. This difference may be used to select the faulty phase. The comparison of the rate of change of δ_{ij-abc} with its predefined minimum value for a defined time interval T will be used to identify power swing. This indicates a stable power swing. It is given as,

$$\Delta\delta_{ij} \geq \Delta\delta_{ij(\min)} \quad t \leq T \quad (8)$$

where δ_{ij} is average of δ_{ij-a}, δ_{ij-b} and δ_{ij-c} If the rate of change of δ_{ij} is greater than the predefined value for more than defined time interval T, it will indicates unstable power swing. It is given as,

$$\Delta\delta_{ij} \geq \Delta\delta_{ij(\min)} \quad t \geq T \quad (9)$$

From (4), the change in impedance seen by the relay is compared with the threshold values set for all three zones. The threshold value for zone-1, zone-2, and zone-3 are ΔZ_1, ΔZ_2, and ΔZ_3 respectively. There might be a possibility that the impedance ΔZ_{ij} can be less than set threshold values if a power swing occurs. Therefore, to discriminate against the condition of fault and power swing, the change in current ΔI_{ij} is determined from (2). If this change in current tends to zero means there is no fault in line but the change in impedance seen by the relay ΔZ_{ij} is due to power swing. This feature is incorporated in protection relays to avoid false tripping.

The system stability factor is defined as a difference of maximum angular separation $\delta_{ij(\max)}$ and actual δ_{ij}.

$$SSF = \delta_{ij\,(\max)} - \delta_{ij} \quad (10)$$

The objective of this research work is to improve the performance of existing SIPS considered for the performance evaluation in this study. It came to know from (1) to (10) that, the unwanted tripping of transmission lines can be prevented by correctly distinguishing the faults from power swings. Therefore, proper actions are initiated to avoid the (i) excess load shedding and (ii) unwanted back down of generating units by considering the practical system conditions. The available lightly loaded transmission lines could be used to achieve this. PMU data is used to determine the loading of each transmission line.

Let N and M are the maximum EHV AC and HVDC transmission lines respectively either approaching or emanating

from the substation. Thus the maximum power transmission capacity for these lines could be expressed as,

$$P_{AC\ \max} = \sum_{j=1}^{N} P_{AC}(j)(\text{for EHV AC lines}) \quad (11)$$

$$P_{DC\ \max} = \sum_{k=1}^{M} P_{DC}(k)(\text{for HVDC lines}) \quad (12)$$

If the actual EHV AC and HVDC transmission lines in operation are $n \leq N$ and $m \leq M$ respectively, the available transformation by these lines are given as

$$P_{AC} = \sum_{j=1}^{n} P_{AC}(j)(\text{for EHV AC lines}) \quad (13)$$

$$P_{DC} = \sum_{k=1}^{m} P_{DC}(k)(\text{for HVDC lines}) \quad (14)$$

The under loading factors in percentage are determined as given in (15) and (16) for EHV AC and HVDC transmission lines respectively.

$$UF_{AC} = \frac{P_{AC\ \max} - P_{AC}}{P_{AC\ \max}}.100 \quad (15)$$

$$UF_{DC} = \frac{P_{DC\ \max} - P_{DC}}{P_{DC\ \max}}.100 \quad (16)$$

These under loading factors will be helpful to maintain system integrity by minimizing the generation unit back downs and thereby avoiding unnecessary load shedding. The above discussed mathematical statements are used to build the proposed algorithm.

SIPS are designed based on power system analysis by defining requirements that they must meet. They are made based on a power system's response to the recorded events or congestions, security assessment, heuristic methods, and AC power flow analysis. SIPS measured electric variables (such as voltage, frequency, etc.) and initiate their protective actions when the contingency has caused the measured value to hit the trigger level. Event-based SIPS are designed to operate upon the recognition of a particular combination of events (such as the loss of several lines in a substation). A general block diagram to provide the proposed system overview is shown in Fig. 7(a).

The power system states reflected in the proposed algorithm is shown in Fig. 7 (b). This algorithm incorporated with existing SIPS is divided into three stages. In stage 1, the algorithm all the time checks if the normal or secure state is maintained and if some disturbance gets detected, it enters stage 2 which is an abnormal or insecure state. It computes the % under-loading capacity of every transmission line. It is used to discriminate among power swing and fault conditions. It blocks the distance relays if the power swing exhibits otherwise it initiates a trip command to the respective circuit breakers. In the third stage, the SIPS operations are carried out

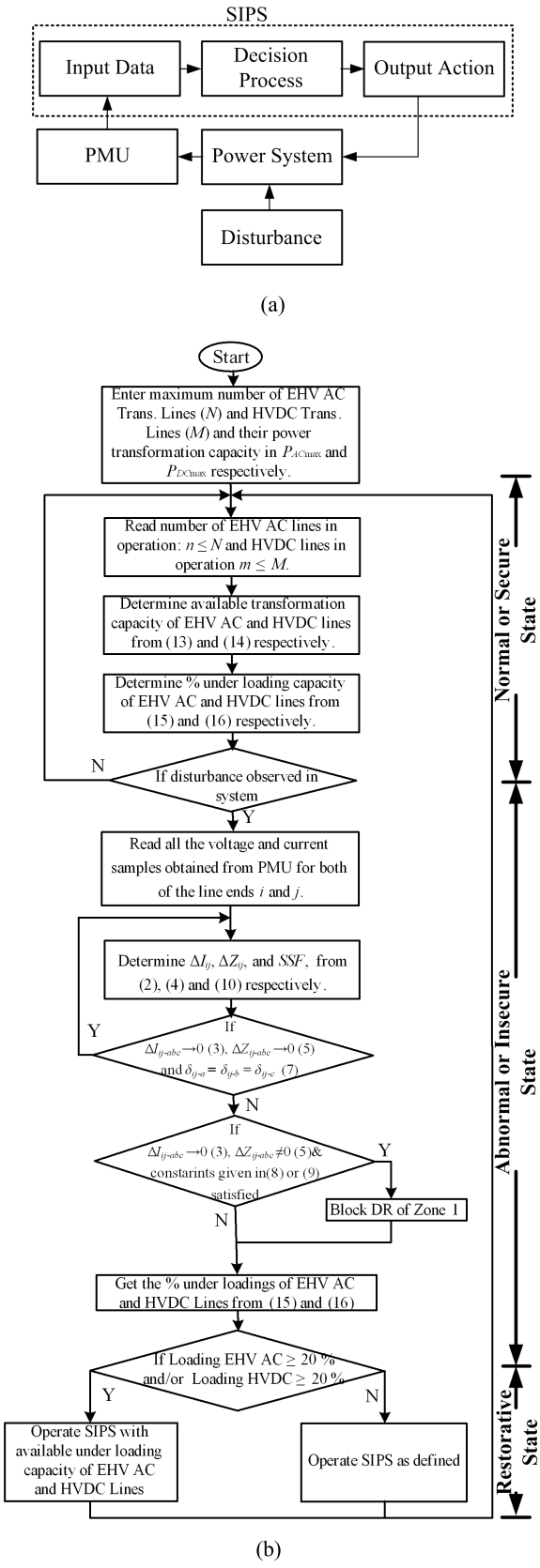

FIGURE 7. System integrity protection scheme (a) General block diagram, and (b) Proposed algorithm.

as defined in Tables 2, 3, and 4 if the lines are under loaded ($\geq 20\%$). For more loading conditions, the SIPS operates with the determined available capacity of transmission lines.

A decision has been taken to restore the normal state by operating the respective SIPS. The possibility of returning to a normal state without restorative action is if the controller selects the options having under loading capacity. In this study, efforts are made to simulate similar conditions that appear in practical cases. Three events discussed in Section II were created and their performance evaluation is done. It is seen that testing of these three events satisfactorily gets performed on IEEE 39-bus New England System. The operational experience carried out in MATLAB and the simulation results are checked with practical events. Further, the algorithm is proposed to overcome the drawbacks of existing SIPS. The performance of this algorithm is tested in MATLAB and validated in ETAP. The performance evaluation is discussed in the following section.

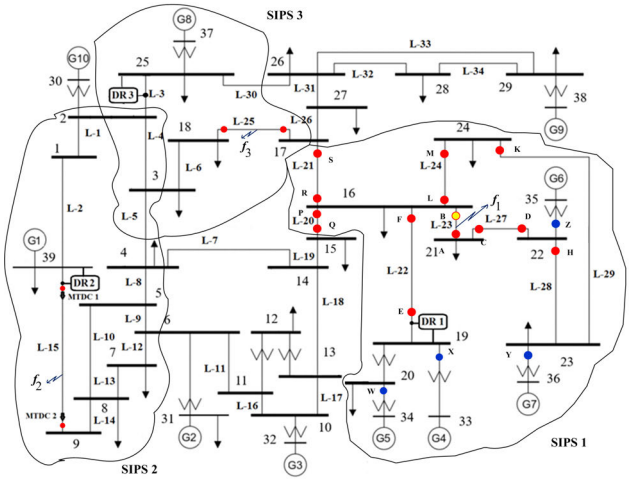

FIGURE 8. IEEE 39-bus New England system embedded with HVDC link.

IV. CASE STUDIES

Responses of three SIPS discussed in the above section are meticulously tested on the IEEE 39-bus New England system embedded with HVDC link. The test system is shown in Fig. 8 consists of 39 buses, 10 generating units, and 19 loads. The buses 30 to 39 are PV buses, as they have connected to power plants, except bus 31 which is referred slack bus, and the rest of the buses are PQ buses. There are 34 transmission lines in this test system. The values are in per unit (pu) of 100 MVA and 345 kV base. The π equivalent circuit is used for the line model. There are 12 transformers in this test system; out of them, 9 are voltage control transformers. The resistances and reactances are expressed in pu of system MVA base and primary bus voltage base. There are 8 tap positions for each transformer. The voltage is controlled on the primary side of the transformer.

A multi-terminal DC (MTDC) system that has more than two converter stations is embedded in this test system.

TABLE 5. Generation and load connected to IEEE 39-bus New England system embedded with HVDC link.

Bus No	Generation		Load	
	P (MW)	Q (MVAR)	P (MW)	Q (MVAR)
3	---	---	320	10
4	---	---	528	60
7	---	---	200	75
8	---	---	407	200
12	---	---	10	80
15	---	---	299	90
16	---	---	330	40
18	---	---	160	30
20	---	---	630	100
21	---	---	270	120
23	---	---	250	100
24	---	---	310	90
25	---	---	220	50
26	---	---	140	20
27	---	---	280	-80
28	---	---	210	30
29	---	---	290	40
31	---	---	10	5
32	650	210	---	---
33	595	-80	---	---
34	510	170	---	---
35	650	220	---	---
36	560	110	---	---
37	515	185	---	---
38	830	40	---	---
39	1000	100	1100	250

The system is built-in MATLAB. Initially, the power flow is examined to verify the validity of the data. The generation and load connected to the respective buses are given in Table 5. The standard procedure for dynamics simulation is followed. Thereafter, the voltage stable and unstable cases are simulated by varying the load levels. Once the simulations are performed, the operational performances of three SIPS are evaluated on the distance relays DR1, DR2, and DR3 respectively.

The secondary frequency control, which is called load frequency control (LFC) or automatic generation control (AGC), is responsible for regulating the frequency in power systems and has two main goals: (i) maintaining the frequency into a desirable range; and (ii) controlling the interchange power through major tie-lines. Therefore, the LFC scheme basically incorporates an appropriate control system for an interconnected power system, which is having the capability to bring the frequencies of each area and the tie line powers back to original setpoint values or very nearer to setpoint values effectively after the load change. This is achieved in this study by the conventional controllers. Simulations are

based on detailed dynamic models of conventional generation units, demand, and an under-frequency load shedding (UFLS) mechanism. Each model of conventional generator consists of a dynamic model of the prime mover (i.e., hydro or thermal, according to the unit type), electric generator (i.e., synchronous machine), the speed governor, generic exciter, and the associated automatic voltage regulation (AVR). The synchronous machine's model is a sixth-order state-space model from the Sim-Power-System toolbox.

Several methodologies are applied to split the power system into smaller islands are based on the slow coherency theory. The slow coherency technique is used to group both generators and load buses into a single group considering the closeness of each other. This approach uses the slow *eigenbasis* theory to collect coherent groups. However, because of the loosely coherent generators and physical constraints, the islands formed change slightly based on location and severity of the disturbance, and loading conditions [36]. Hence, the slow-coherency theorem to generate a database of tightly and loosely coupled generators is not considered in this work.

All generators are equipped with droop controllers to implement primary frequency regulation. The generators only implement primary frequency control. The regulation (droop) coefficients for all the generators are 5%. UFLS relays are implemented to curtail loads when the system frequency falls below a certain level. Loads are shed proportionally to the frequency drop. The load shedding steps are (a) 1.0 Hz to 1.2 Hz shed 5% of load, (b) 1.2 Hz to 1.4 Hz shed 15 % of load, (c) 1.4 Hz to 1.6 Hz shed 25% of load, (d) 1.6 to 1.8 Hz shed 35% of load, (e) 1.8 Hz to 2.0 Hz shed 45% of load, and (f) below 2.0 Hz shed 50% of the load. UFLS is implemented in all the 19 aggregated loads. It uses PMUs to measure frequency for the UFLS scheme. All the UFLS relays implement a 0.15∼ second delay to avoid unnecessary UFLS actions. The frequency threshold values for restoring the loads are 0.25 Hz for full load restoration, 0.5 Hz for restoring 95% of the loads, and 0.75 Hz for 85% restoring.

In this work, the load shedding strategy based on the UFLS relay is preferred and thereby the priority of the loads is classified as critical loads and non-critical loads. The loads connected at bus 3,4,12, 15, 18, 26, and 28 are ranked as critical loads and the rest of the loads are non-critical loads. The system frequency response identified from phasor measurement units is used for the curtailment of a load.

A. PERFORMANCE EVALUATION OF SIPS-1

SIPS-1 is tested without and with the proposed methodology for its capability to forbid system instability under normal and stressed system conditions. The relay at bus 19 for line L-22 at CB location E is quoted as Test Relay 1 (DR1) and it is fixed for its safeguard operation during voltage stress, load encroachment, and power swing.

The IEEE 39-bus New England test system embedded with HVDC link at an early stage was executed in MATLAB.

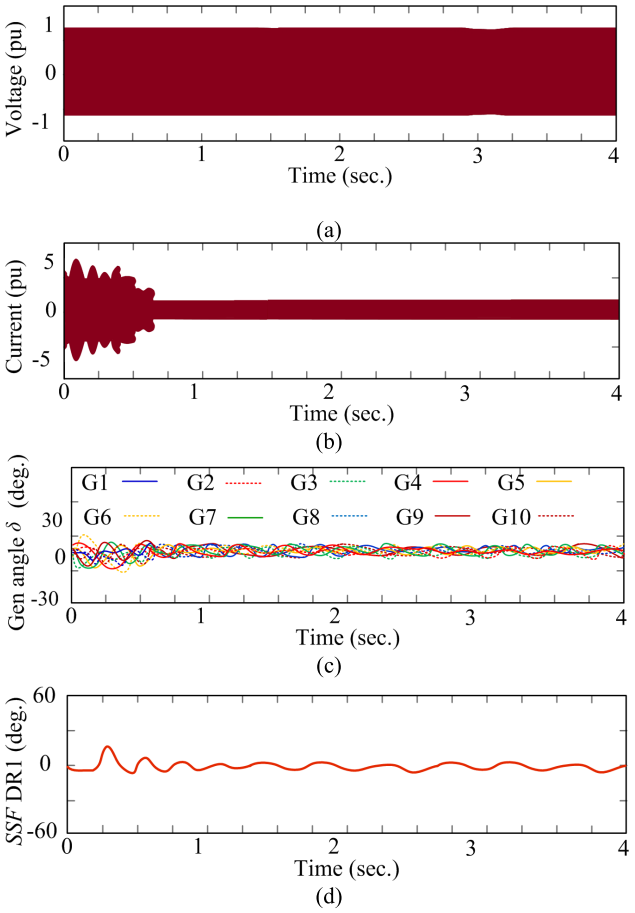

FIGURE 9. Performance evaluation of SIPS-1 under normal condition (a) Voltage in pu observed by DR1, (b) current in pu recorded by DR1, (c) all generating unit's angles variations, and (d) *SSF* between bus 16 and bus 19.

The 31st bus to which G2 is connected is taken as a reference bus and thus the power angle for this bus is zero. The bus voltage, power angle and line power flows are illustrated in Fig. 9 for the normal operating condition. The voltage and currents observed by DR1 are depicted in Fig. 9 (a) and (b) respectively. It is seen from Fig. 9 (c) and (d) that the system is stable and all the generation angles are settled and thereby system stability factor (*SSF*) is also within limits.

To validate the performance, the IEEE 39-bus New England test system embedded with HVDC link was restructured with the help of Electrical Transient Analyzer Program (ETAP) [37]. The system was simulated in ETAP and the results are correlated with MATLAB as shown in Fig. 10. The voltage noticed from Fig. 10 (a) for bus 16 by MATLAB and ETAP are 0.978 pu and 0.985 pu respectively. The power angle for this bus observed from Fig.10 (b) is 5.794 degrees and 5.848 degrees from respective simulations. The active power observed shown in Fig. 10 (c) for line L-23 connected is 193.15 MW and 194.89 MW from MATLAB and ETAP simulations respectively. However, the reactive power flow shown in Fig 10 (d) is 36.22 MVAR and 36.54 MVAR obtained from the respective simulations. Line L-15 is HVDC

line and it carries only active power of 250 MW. It is observed that both the simulation results are matching with each other. In this power system scenario, all the lines are engaged in power transmission.

To produce a power swing in the system, a three-phase symmetrical fault is created in line L-23 which is connecting bus 16 and bus 21. The fault is cleared by tripping the line circuit breakers A and B. By varying the fault clearance time, it is possible to simulate stable and unstable power swings. The concentric circle method is used to check the performance. The time taken by the impedance trajectory to cross exterior and zone-3 circles is used to distinguish power swing from the fault. Time taken threshold value is considered as 25 ms.

1) PERFORMANCE EVALUATION OF SIPS-1 UNDER STABLE POWER SWING CONDITION

The symmetrical three-phase fault (f_1) is enforced at 1 s in the line L-23 when the load connected at bus 24 is (150+j 60) MVA instead of regular load (310+j90) MVA. The fault at both ends cleared in 90 ms after the opening of the circuit breaker at locations A and B. The conditions (5), (8), and (9) are satisfied. It indicates a power swing and there is no fault. The distance relay DR1 detects a power swing in zone-2. The time taken by the impedance trajectory to enter into its zone-1 circle is more than its threshold value. This enables the power swing blocking (PSB) feature of distance relays at locations E, M, S, and Q.

The waveforms of voltage and current indicate a stable power swing shown in Fig. 11 (a) and (b) respectively. The generator angle of G6 is increased momentarily from 8.838 degrees and settled at 9.323 degrees in MATLAB simulation. In ETAP simulation, it varies from 8.894 degrees and settled at 9.381 degrees. There are slight variations observed in generation angles of remaining generating units as seen from Fig. 11 (c). The power swing mitigates after 3.6 sec. The stability curve is depicted in Fig. 11 (d). Line L-23 was tripped and its power flow turned zero. There is a variation in voltage and power angle at all the buses seen from Fig. 12 (a) and (b) respectively. The earlier power flow from L-23 was carried out by adjacent lines as shown in Fig. 12 (c) and (d). The power flow of line L-24, L-28, and L-29 enhance from (188+j16) MVA to (380+j20) MVA, (28+j34) MVA to (220+j70) MVA, and (338+j44) MVA to (530+j80) MVA respectively. However, the power flow of line L-27 was reduced from (462+j156) MVA to (270+j120) MVA. The system remains stable and there is no need for SIPS operation as well as no additional load shedding is required. It is observed that the SIPS-1 operates when the connected load is more than 219 MVA at bus 24. As soon as the fault occurs in line L-23, the connected load at bus 16 curtailed. It imposes load shedding of (310+j90) MVA and accordingly generation back down of unit G6. The change in active and reactive power flow is shown in Fig. 12(e) and (f) respectively. The power flow of line L-24, L-28, and L-29 enhance from (188+j16) MVA to (380+j20) MVA,

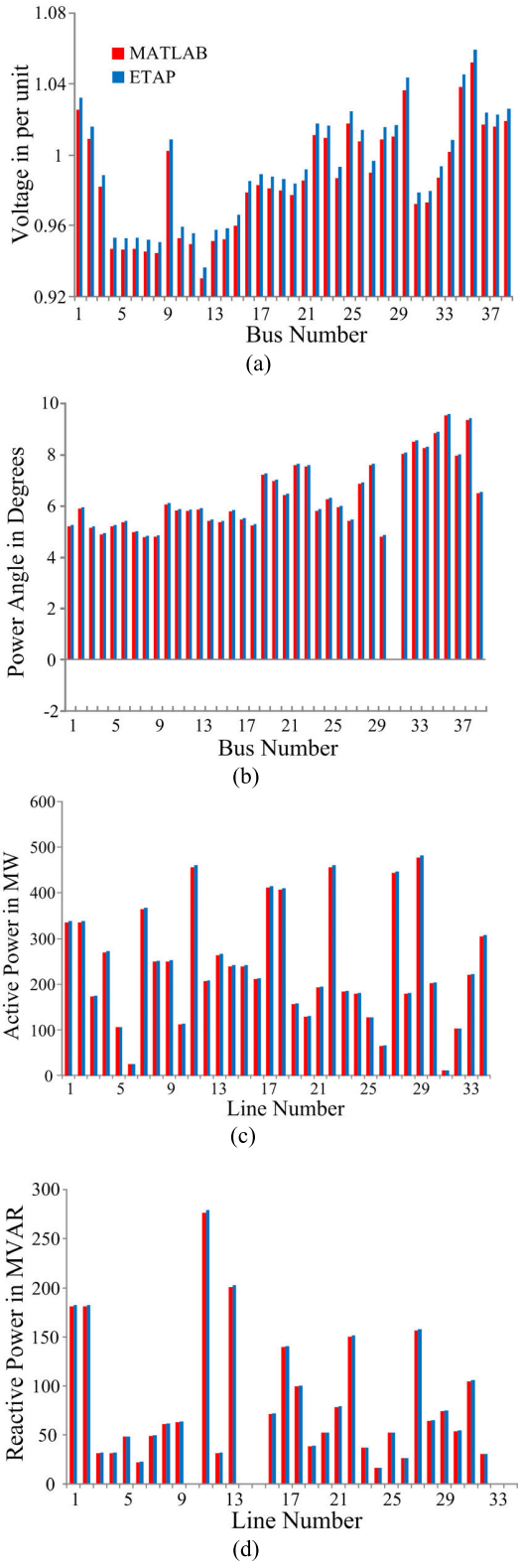

FIGURE 10. Comparative results for normal condition, (a) bus voltage, (b) power angle, (c) active power flow, and (d) reactive power flow.

(188+j64) MVA to (70+j10) MVA, and (498+j74) MVA to (380+j20) MVA respectively. However, the power flow of line L-27 was reduced from (462+j156) MVA to

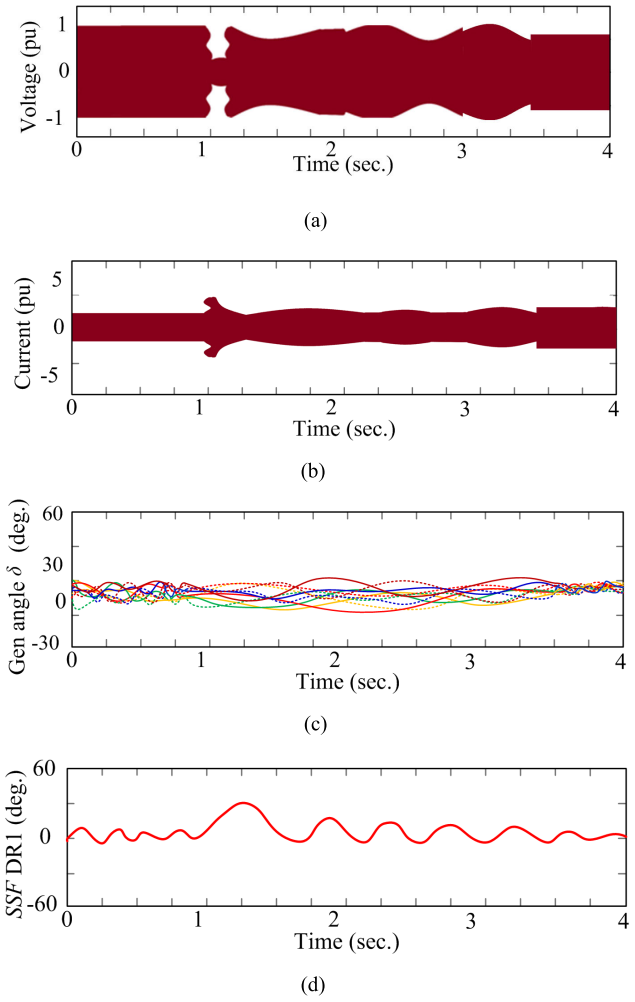

FIGURE 11. Performance evaluation of SIPS-1 under normal condition (a) voltage observed by DR1, (b) current recorded by DR1, (c) all generating unit's angles variations, and (d) *SSF* between bus 16 and bus 19.

(270+j120) MVA. The system is maintained stable but curtailed the load connected at bus 24.

2) PERFORMANCE EVALUATION OF SIPS-1 UNDER UNSTABLE POWER SWING CONDITION

The symmetrical three-phase fault (f_1) is imposed at 1 s in the line L-23. Circuit breaker A operates as it gets a command from the respective relay in zone-1. However, the opening time of circuit breaker B of line L-23 is set high at 260 ms. This is a breaker stuck condition. The time interval is deliberately set high so that the distance relay DR1 experience a power swing in zone-2.

The conditions (5), (8), and (9) are satisfied. It indicates an unstable power swing but there is no fault in zone-1 of the distance relays located at E, M, S, and Q. But all these relays detect power swing in their zone-2. Thus for all these locations, the power swing blocking (PSB) feature is activated. As breaker B got stuck, there should be the operation of local breaker backup (LBB) protection provided to bus 16. Thus, it was intended that the circuit breakers L, F, P, and R should receive the trip command and de-energize bus 16. But LBB protection was not in service. The impedance trajectory enters into zone-1 of relays located at E, M, S, and Q, and the constraints (5), (8), and (9) are not satisfied. The fault is reflected in this zone along with the power swing. This unblocks the relays at locations E, M, S, and Q. DR1, initiate a trip command to breaker E. Similarly, the respective breakers of the remote end connected to bus 16 i.e. circuit breakers M, Q, and S got tripped because of the imposition of power swings and unclear fault in their respective zone-2. This de-energized bus 16 and curtailed connected load of (330+j40) MVA. This tripping causes no path for power evacuation from generator G4, G5, G6, and G7. The loads connected at bus 20, 21, 23, and 24 are not matching with excessive generation under such circumstances. Therefore, all these generators tripped due to out of step or over frequency protection.

An unstable power swing in voltage and current waveforms is shown in Fig. 13 (a) and (b) respectively. The angular dissociation between rotor angles of alternators and repeated oscillations clearly pinpoint unstable power swing as given in Fig.13 (c). The *SSF* curve tending towards instability is given in Fig. 13 (d). The system became unstable after 3.8 sec. This causes the entire blackout occurred in the corresponding region. As soon as bus 16 disconnected from the system, its voltage became zero. This not only causes blackouts in the specified region but also changes the voltages and power angles at other buses as shown in Fig. 14 (a) and (b) respectively. The change in the active and reactive power flow in the rest of the system is shown in Fig. 14 (c) and (d) respectively.

In the existing logic, the power swing blocking scheme implemented was 'block all zones except zone-1' on power swing. Circuit breaker A opened correctly as the fault observed in zone-1. However, this SIPS-1 failed due to (i) non-opening of breaker B for line L-23, (ii) no operation of LBB at bus 16 (iii) power swings which were earlier seen in zone-2 did not get mitigated as the fault was not cleared (iv) it entered into zone-1 for distance relays located at E, M, Q, and S cause opening of respective circuit breakers because of fault in zone-2, (v) circuit breakers W, X, Y, and Z tripped due to over frequency protection. Based on this performance evaluation, the discrepancy in the existing SIPS is modified by applying the proposed algorithm. The modification is given in the following subsection.

3) PERFORMANCE EVALUATION OF SIPS-1 UNDER STABLE POWER SWING WITH THE PROPOSED ALGORITHM

The power system is operating under the condition as shown in Fig. 10. All the lines are under operation. At 1 sec, symmetrical three-phase fault (f_1) is enforced over the line L-23. This line was carrying 192 MW and 36 MVAR.

The fault was cleared in 90 ms. Test relay DR1 observed power swing in zone-2. There was no fault in zone-1. This satisfies the conditions (5), (8), and (9). Thus, the SIPS enables the power swing blocking (PSB) feature of distance relays at

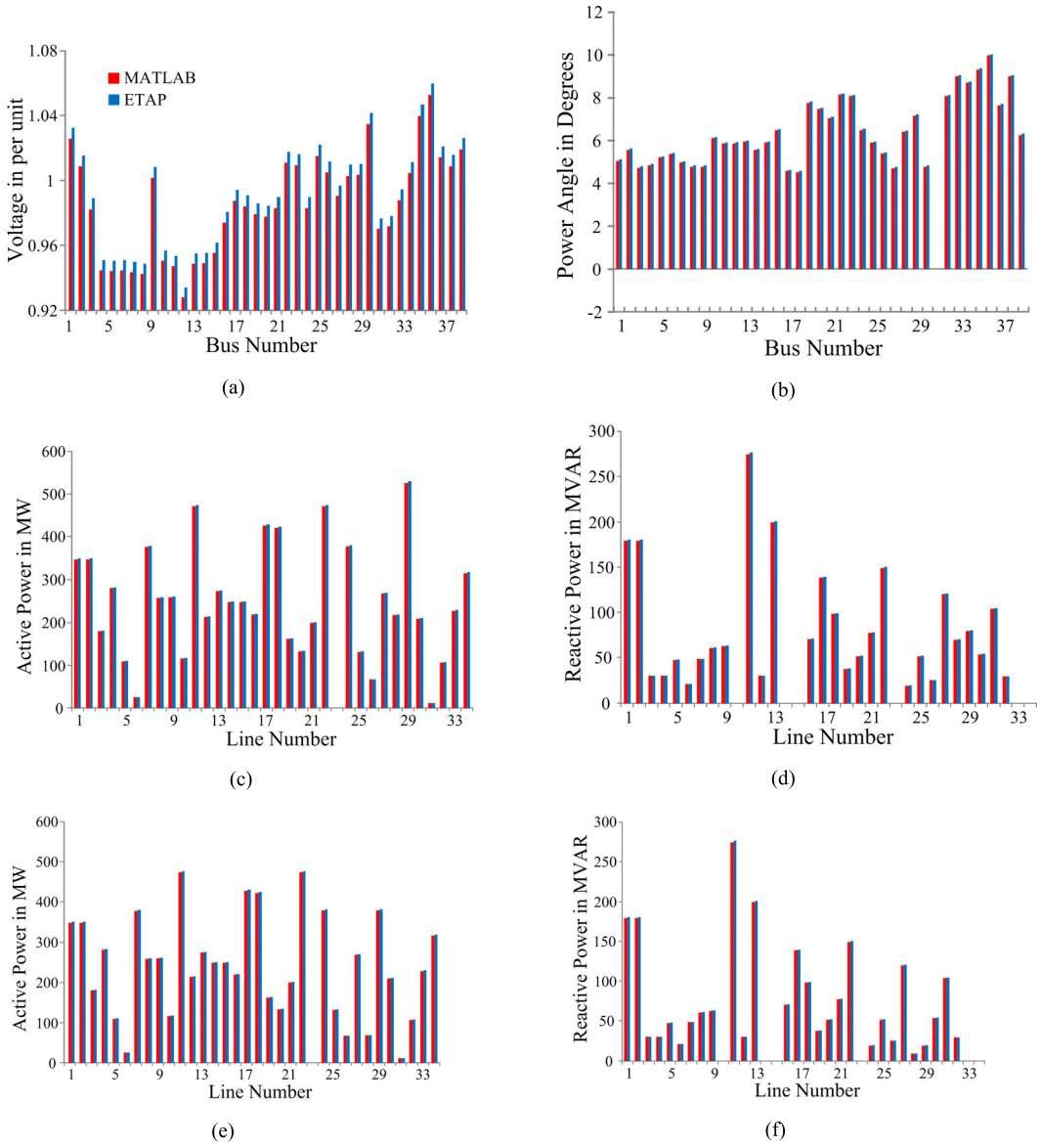

FIGURE 12. Performance of IEEE 39-bus system under the stable condition when line L-23 tripped (a) bus voltage, (b) power angle, (c) active power flow, (d) reactive power flow, (e) active power flow SIPS-1 operated, and (f) reactive power flow SIPS-1 operated.

locations E, M, S, and Q. It implies load shedding of 310 MW and 90 MVAR on bus 24. As the line L-23 is not available, its flow was diverted by lines L-24, L-28, and L-29. The system remains stable due to load curtailment. Lines L-24, L-28, and L-29 are operated at 63.5%, 11.84%, and 36.5% respectively of their rated capacity. It means these lines can deliver more power and thereby the load shedding shall be reduced.

The proposed algorithm came into action and imposes load shedding of 101 MW only. This avoids the load shedding of all load connected on bus 24. It is possible to supply (209+j90) MVA load on this bus. The power transfer by L-29 is reached at 599 MVA. The waveforms of voltage and current indicate a stable power swing shown in Fig. 15 (a) and (b) respectively.

Slight variations observed in generation angles of remaining generating units as seen from Fig. 15 (c). The power swing mitigates after load curtailment at 3.71 sec. The stability curve is shown in Fig. 15 (d). As the line L-23 was tripped and thus its power flow turned zero. Variation in voltage and power angle at all the buses given in Fig. 16 (a) and (b) respectively. Power flows are shown in Fig. 16 (c) and (d). The system remains stable due to the SIPS operation which enforced required load shedding.

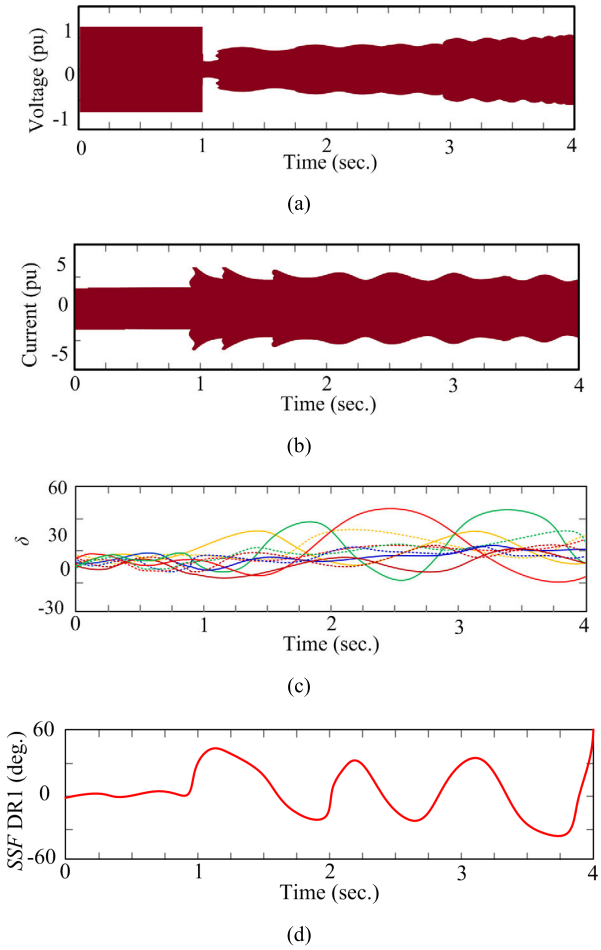

FIGURE 13. Performance evaluation of SIPS-1 under unstable condition (a) voltage observed by DR1, (b) current recorded by DR1, (c) all generating unit's angles variations, and (d) *SSF* between bus 16 and bus 19.

4) PERFORMANCE EVALUATION OF SIPS-1 UNDER UNSTABLE POWER SWING WITH THE PROPOSED ALGORITHM

With the improvement in measurement technologies, the outright rotor angle is now assessable using the PMU signal as input and is declared to be useful in correcting power system vigorous performance. For an aberrant contingency, the eminence of the generation angle and its change are higher than a balanced contingency. For the IEEE 39-bus system, an unstable squabble is detected by DR1 when the symmetrical fault is kept under the hanged condition over line L-23. It illustrates that the system is near instability, curative actions are originated and the system instability is annexed. While ratifying this reformed scheme; it has been taken care to secure that the protection relay is encouraged for the operation of every fault during power swing.

The symmetrical fault (f_1) is applied on the line L-23 while power swing, at 1 s. This fault is cleared after 85 ms by circuit breaker A but breaker B got stuck. Relay DR1 located at E as well as relays at locations M, Q, and S detect the fault in zone-2 during power swing. The proposed algorithm is incorporated in the SIPS-1 at the start and based on *SSF* the

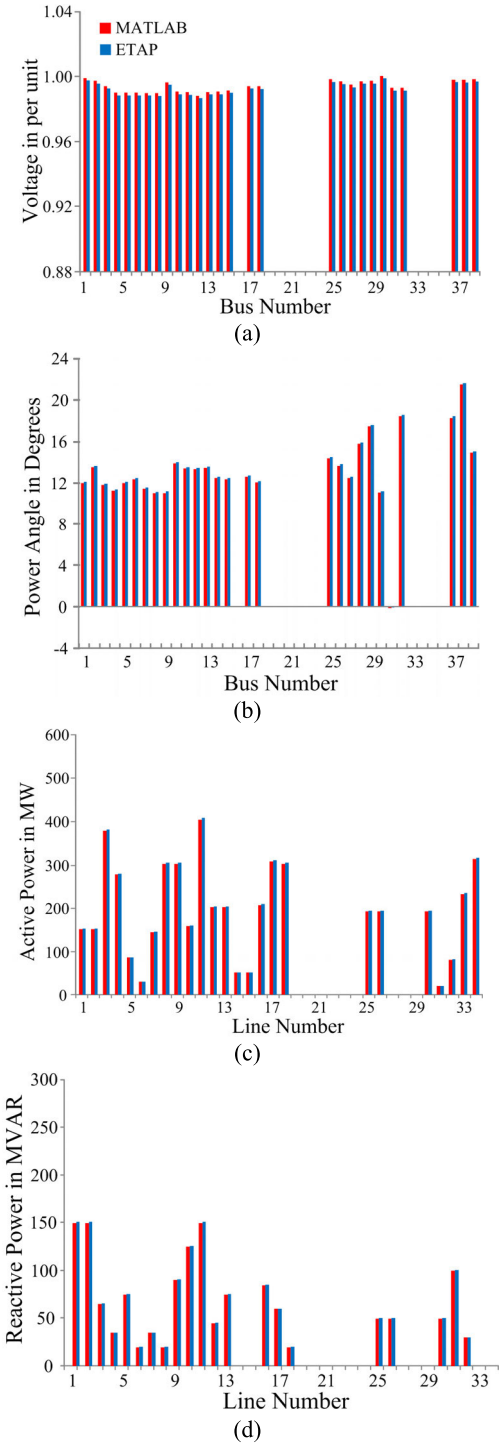

FIGURE 14. Performance of IEEE 39-bus system under the unstable condition when line L-23 fault was not cleared (a) bus voltage, (b) power angle, (c) active line power, and (d) reactive line power.

corresponding distance relays concerning CB locations E, M, Q, and S are de-blocked.

These relays issue trip commands to corresponding circuit breakers and disconnect bus 16 from the system. It is considered that LBB protection of bus 16 is out of service. The modification made in SIPS is such that whenever either line

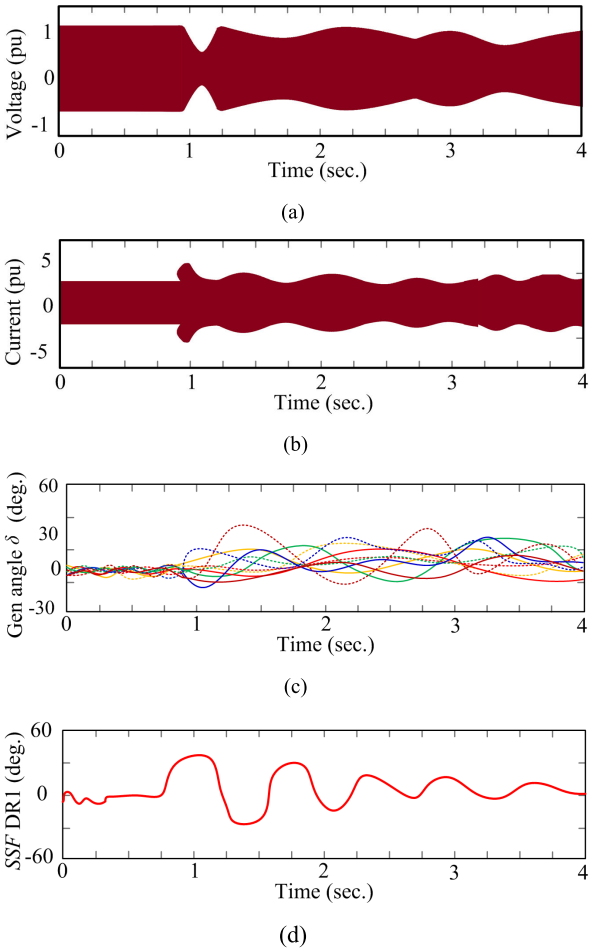

FIGURE 15. Performance evaluation of SIPS-1 with proposed algorithm under stable power swing (a) voltage observed by DR1, (b) current recorded by DR1, (c) all generating unit's angles variations, and (d) *SSF* between bus 16 and bus 19.

L-22 trip or bus 16 is disconnected, then the generating unit G4 gets detached from the system. Under such contingency conditions, generator G4 is taken out from service, and generation of G5, G6, and G7 need to be backing down in proportion to load at bus 20, 22, and 23. This prevents unwanted tripping of generator G5, G6, and G7 at over frequency condition. This not only mitigates the power swing observed by protection relays but also avoids the entire blackout in this region. Thus, the system acquires stable conditions as shown in Fig. 17 (a), (b), (c) and (d) respectively for the voltage, current, power angle, and *SSF*. The angular displacement observed is greater than 28.1 degrees or $\pi/6.4$ radians. Whereas, lines flow after discharging of bus 16 are shown in Fig. 18 (a), (b), (c) and (d) for the bus voltage, power angle, and active/reactive power respectively. The proposed algorithm determines the under loading factor (UFAC) of lines L-17, L-18, and L-19 as 48.16%, 49.83%, and 100% respectively. Hence, the load shedding at bus 14 is partially withdrawn. Under such a power system scenario, the entire load of bus 27 is curtailed but the system can supply (139.87+j64.13) MVA load at bus 15 due to effective power management by the proposed algorithm.

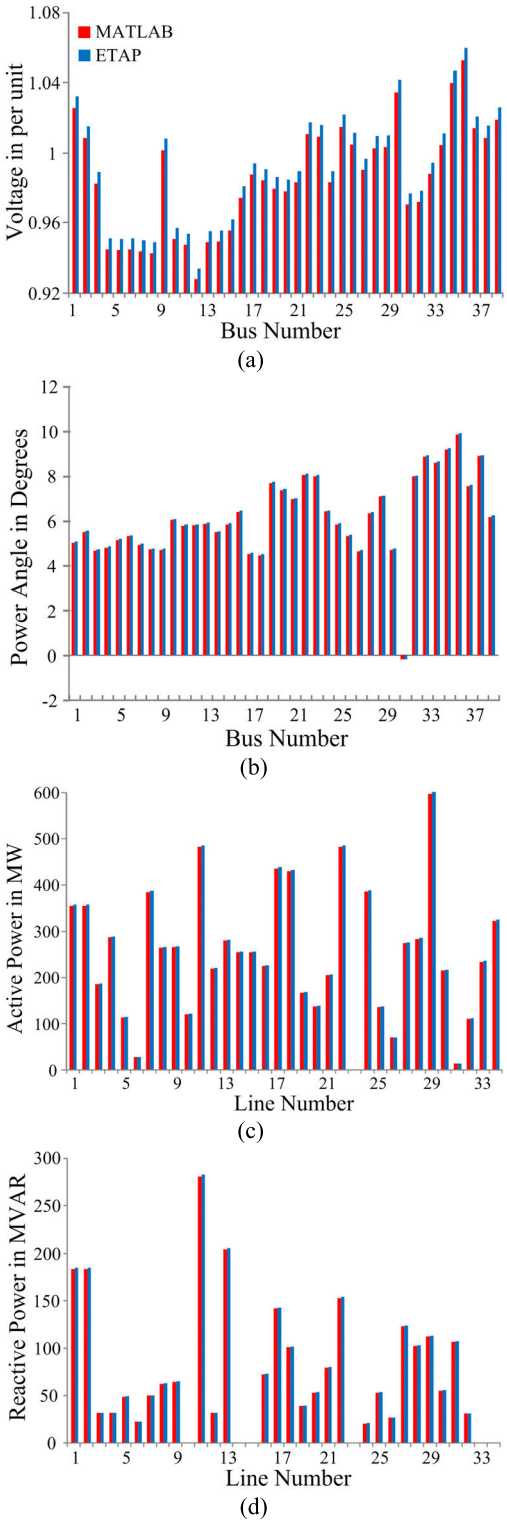

FIGURE 16. Performance of IEEE 39-bus system under stable power swing and SIPS-1 operated with proposed algorithm (a) bus voltage, (b) power angle, (c) active power flow, and (d) reactive power flow.

Based on these operational evaluation results, the following are the recommendations for the SIPS-1 functioning at CGPL. (i) Check the settings of all the distance relays and coordinate their gradation properly, (ii) Ensure that bus-bar

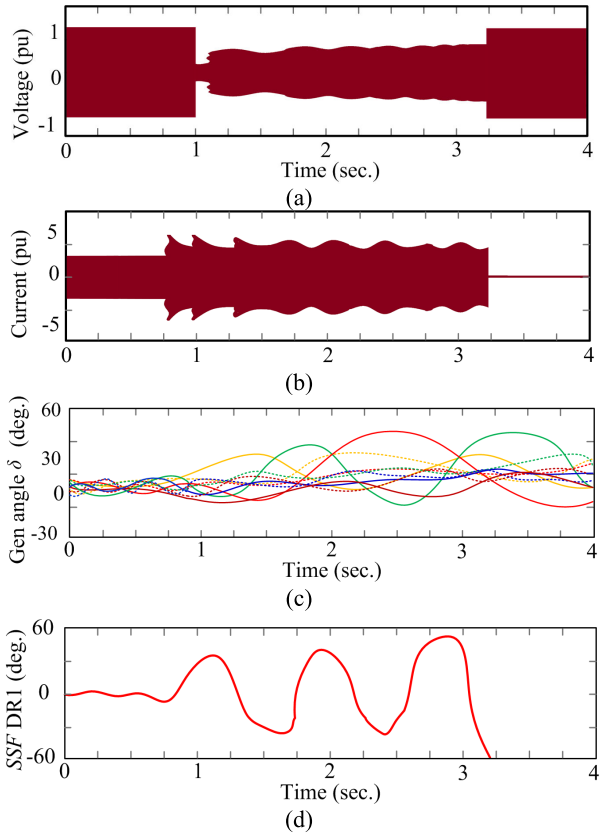

FIGURE 17. Performance evaluation of SIPS-1 with proposed algorithm under unstable power swing (a) voltage observed by DR1, (b) current recorded by DR1, (c) all generating unit's angles variations, and (d) *SSF* between bus 16 and bus 19.

and LBB protections are in operation (iii) Determine the loading factor of every line and maintain the power flow accordingly, (iv) Disconnect the unwanted generating units and avoid operation of over frequency protection under contingency conditions. This prevents the disconnection of the remaining generating unit from the system, (v) Manage back down of generation by frequency load dropping characteristics at every generation end.

B. PERFORMANCE EVALUATION OF SIPS-2 WITH PROPOSED METHODOLOGY

The symmetrical fault (f_2) was applied at 2 s in the DC line L-15, between bus 9 and bus 39 when the line was carrying 580 MW and load at bus 39 was (770+j180) MVA.

Circuit breaker opening at both ends in 80 ms clears the fault. As an effect of the symmetrical fault, the test relay DR2 diagnoses a power swing momentarily. This tripping enhanced the power flow of lines L-4 and L-12 by more than 600 MVA. The maximum allowable power transmission is restricted to 600 MVA for 400 kV due to its thermal limits. Thus the SIPS came into operation and curtailed load connected at bus 7. It also backs down generation G2 to (200 +j75) MVA. The performance of this SIPS-2 is shown in Fig. 19. The voltage and current waveforms are depicted

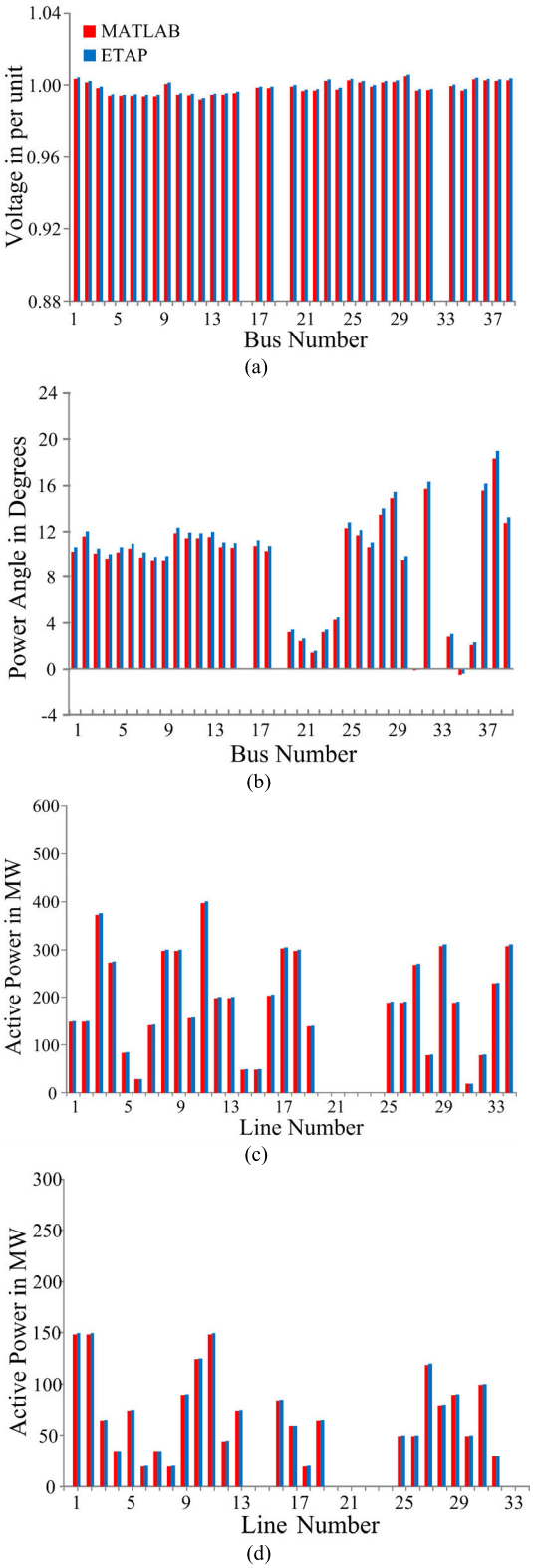

FIGURE 18. Performance of IEEE 39-bus system under unstable power swing and SIPS operated with proposed algorithm (a) bus voltage, (b) power angle, (c) activ line power, and (d) reactive line power.

in Fig. 19 (a) and (b) respectively. The angular segregation of generator rotor angles and the stability curve are shown in Fig 19 (c) and (d) respectively.

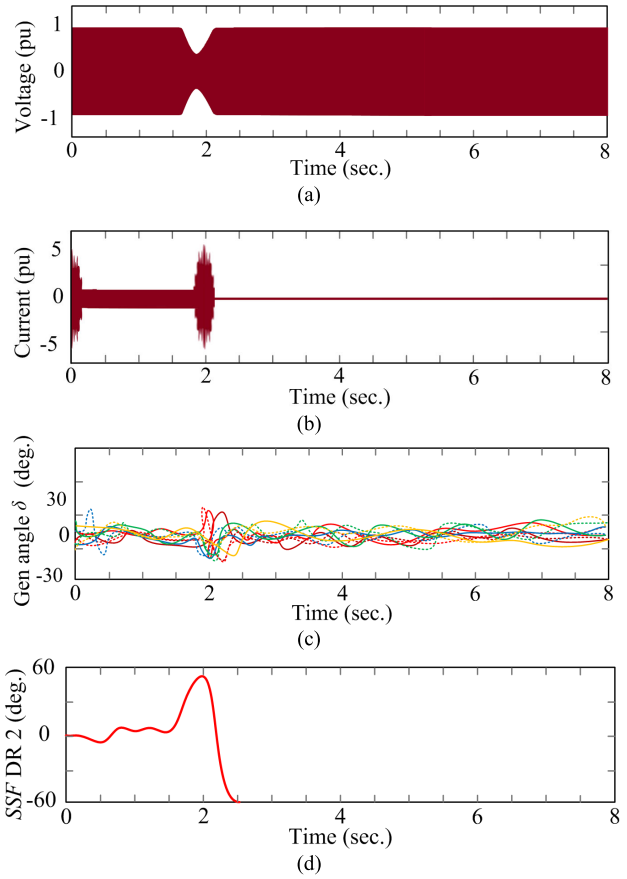

FIGURE 19. Performance evaluation of SIPS-2 (a) voltage observed by DR2, (b) current recorded by DR2, (c) all generating unit's angles variations, and (d) *SSF* between bus 9 and bus 39.

The proposed algorithm determines the underloaded adjacent lines. It is observed that a line L-12 is 27.57% underloaded. Therefore, the control action improves the generation back down of G2 by 100.1 MW and also reduced the load shedding at bus 8 by 99.3 MW. The comparative results for some buses and lines among MATLAB and ETAP simulations without and with the application of the proposed algorithm are shown in Fig. 20.

It is seen from Fig. 20 (a) and (b) that as the generation back down is reduced, it not only results in the improvement of bus voltages but also minimizes the angular disturbance. The improvement in active and reactive power flow is shown in Fig. 20 (c) and (d) respectively.

C. PERFORMANCE EVALUATION OF SIPS-3 WITH PROPOSED METHODOLOGY

The symmetrical fault (f_3) applied at 2 s in the line L-25 joined with bus 17 and bus 18 when this line was carrying 530 MW. Line L-6 importing power towards bus 3 from bus 18. Circuit breaker opening at both ends in 83 ms clears the fault. As an effect of the symmetrical fault, the test relay DR3 diagnoses a power swing momentarily. This tripping

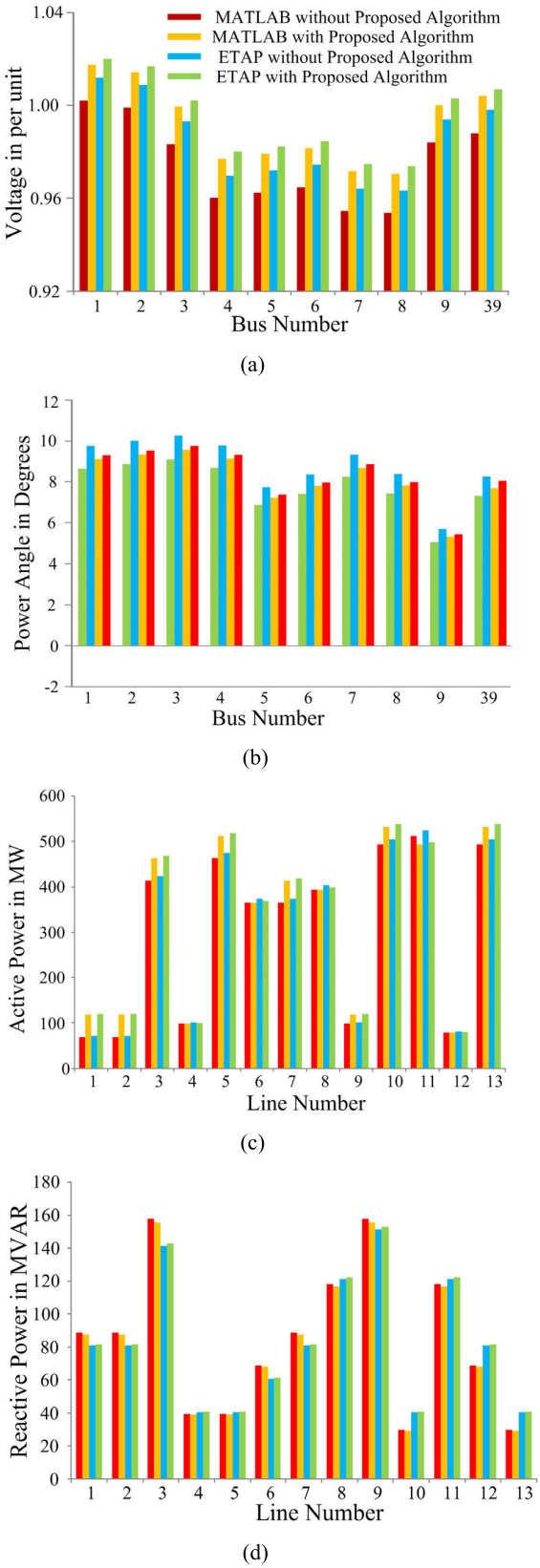

FIGURE 20. Comparative results for SIPS-2 without and with the application of proposed algorithm (a) bus voltage, (b) power angle, (c) active power flow, and (d) reactive power flow.

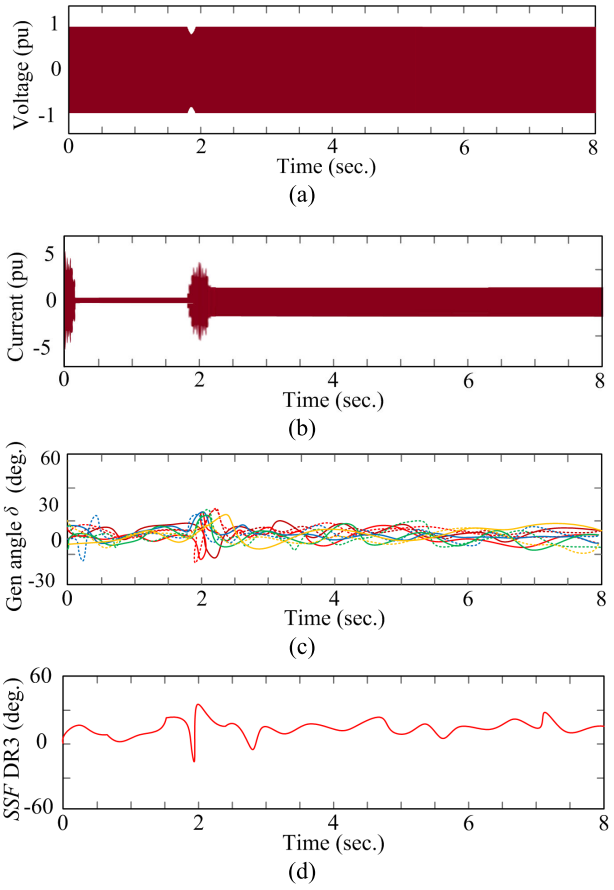

FIGURE 21. Performance evaluation of SIPS-3 (a) voltage observed by DR3, (b) current recorded by DR3, (c) all generating unit's angles variations, and (d) *SSF* between bus 2 and bus 25.

enhanced the power flow of lines L-3 and L-4 by more than 600 MW. Thus the SIPS came into operation and started to back down generation G8 by 350 MW. It curtailed the complete load at bus 18 and preserved 122 MW load at bus 3. The performance of this SIPS-3 is shown in Fig. 21. The voltage and current waveforms are depicted in Fig. 21 (a) and (b) respectively. The angular segregation of generator rotor angles and the stability curve are shown in Fig 21 (c) and (d) respectively.

The loading factor was determined as 21.62 % for line L-3 and 30 % for line L-4. Therefore, control action back down the generation of G1 to 100 MW and also reduced load shedding at bus 3 by 40 MW. It also avoids the complete curtailment of load at bus 18 and maintained 80 MW load. The comparative results for some buses and lines among MATLAB and ETAP simulations without and with the application of the proposed algorithm are shown in Fig. 22. It is seen from Fig. 22 (a) and (b) that as the generation back down is reduced, it not only results in the improvement of bus voltages but also minimizes the angular disturbance. The improvement in active and reactive power flow is shown in Fig. 22 (c) and (d) respectively. The outcome of this paper is as below.

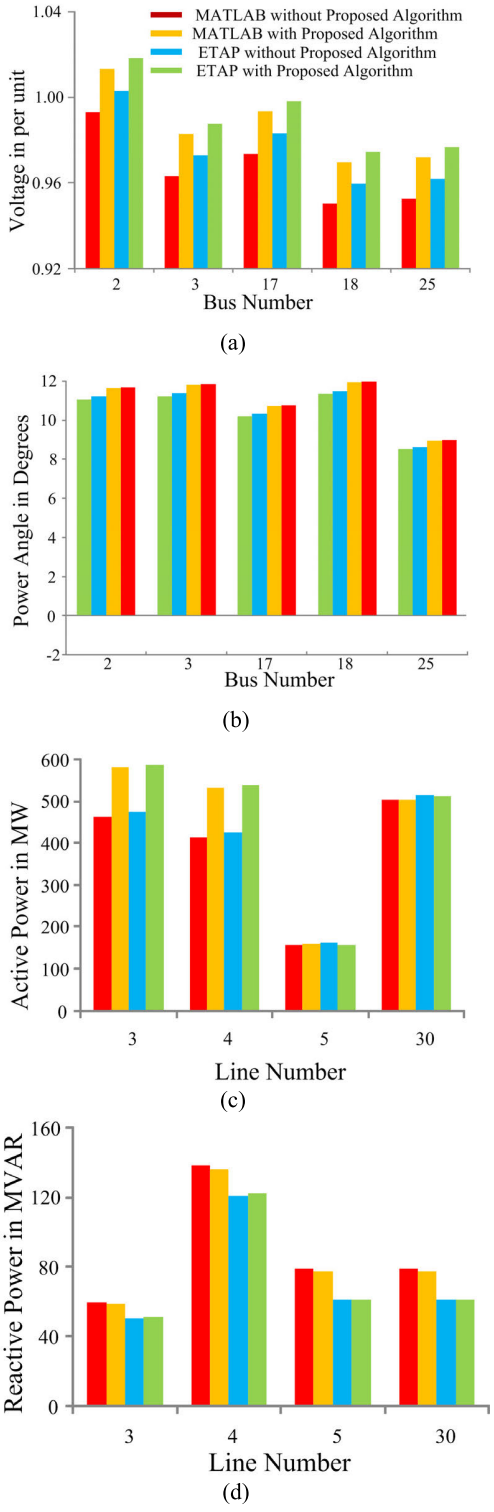

FIGURE 22. Comparative results for SIPS-3 without and with the application of proposed algorithm (a) bus voltage, (b) power angle, (c) active power flow, and (d) reactive power flow.

i. Analysis of three different SIPS is carried out in simulation with the commercially available software MATLAB on the 39-bus New England system embedded with an HVDC link.

ii. Performance evaluation emphasized causes for the correct or incorrect operation of existing SIPS.
iii. An algorithm is proposed which requires PMU data to decide blocking and de-blocking of distance relays so that the existing SIPS could be operated effectively.
iv. The proposed scheme does not require any estimation or prediction methodology and it will be more effective for critical application.
v. Modification due to the proposed algorithm not only makes effective use of generating units by back down the generation but also avoids maximum load shedding.
vi. Results obtained in MATLAB platforms are validated with the results of ETAP and found satisfactory.

V. CONCLUSION

This paper presents three case studies based on the operational experience of important SIPS in India. The drawbacks in the execution of existing SIPS are overcome by proposing an algorithm. The actual time data from PMU will knock out the requirement for complex system modeling and the possibility of potential errors. The algorithm separates the power swing and fault conditions and avoids unwanted tripping. It also identifies the underloaded AC and DC lines and thereby avoids excessive load shedding. The strenuous simulations executed in MATLAB and ETAP over the IEEE 39-bus New England system embedded with HVDC link convince the materiality of the proposed algorithm in assuring system integrity.

REFERENCES

[1] A. G. Phadke and J. S. Thorp, *Synchronized Phasor Measurements and Their Applications*. New York, NY, USA: Springer, 2008.
[2] S. Ghosh, D. Ghosh, and D. K. Mohanta, "Situational awareness enhancement of smart grids using intelligent maintenance scheduling of phasor measurement sensors," *IEEE Sensors J.*, vol. 17, no. 23, pp. 7685–7693, Dec. 2017.
[3] A. G. Phadke and T. Bi, "Phasor measurement units, WAMS, and their applications in protection and control of power systems," *J. Mod. Power Syst. Clean Energy*, vol. 6, no. 4, pp. 619–629, Jul. 2018.
[4] J. Giri, M. Parashar, J. Trehern, and V. Madani, "The situation room: Control center analytics for enhanced situational awareness," *IEEE Power Energy Mag.*, vol. 10, no. 5, pp. 24–39, Sep. 2012.
[5] G. Rietveld, J.-P. Braun, R. Martin, P. Wright, W. Heins, N. Ell, P. Clarkson, and N. Zisky, "Measurement infrastructure to support the reliable operation of smart electrical grids," *IEEE Trans. Instrum. Meas.*, vol. 64, no. 6, pp. 1355–1363, Jun. 2015.
[6] P. M. Anderson and B. K. LeReverend, "Industry experience with special protection schemes," *IEEE Trans. Power Syst.*, vol. 11, no. 3, pp. 1166–1179, Aug. 1996, doi: 10.1109/59.535588.
[7] C. W. Taylor, D. C. Erickson, K. E. Martin, R. E. Wilson, and V. Venkatasubramanian, "WACS-Wide area stability and voltage control system: R&D and online demonstration," in *Proc. IEEE*, vol. 93, no. 5, pp. 892–906, May 2005, doi: 10.1109/JPROC.2005.846338.
[8] F. Chunju, D. Xiuhua, L. Shengfang, and Y. Weiyong, "An adaptive fault location technique based on PMU for transmission line," in *Proc. IEEE Power Eng. Soc. Gen. Meeting*, Tampa, FL, USA, Jun. 2007, pp. 1–6, doi: 10.1109/PES.2007.385545.
[9] E. O. Schweitzer, A. Guzman, H. J. Altuve, D. A. Tziouvaras, and J. Needs, "Real-time synchrophasor applications in power system control and protection," in *Proc. 10th IET Int. Conf. Develop. Power Syst. Protection (DPSP). Manag. Change*, Manchester, U.K., 2010, pp. 1–5, doi: 10.1049/cp.2010.0343.
[10] W. Gao and J. Ning, "Wavelet-based disturbance analysis for power system wide-area monitoring," *IEEE Trans. Smart Grid*, vol. 2, no. 1, pp. 121–130, Mar. 2011, doi: 10.1109/TSG.2011.2106521.
[11] M. Korkali, H. Lev-Ari, and A. Abur, "Traveling-wave-based fault-location technique for transmission grids via wide-area synchronized voltage measurements," *IEEE Trans. Power Syst.*, vol. 27, no. 2, pp. 1003–1011, May 2012, doi: 10.1109/TPWRS.2011.2176351.
[12] E. Hillberg, F. Trengereid, Ø. Breidablik, K. Uhlen, G. KjØlle, S. LØvlund, J.O. Gjerde, "System integrity protection schemes—Increasing operational security and system capacity," *Proc. CIGRE*, Paris, France, vol. 21, 2012, pp. 1–5. [Online]. Available: http : //www.cigre.org
[13] M. Panteli, P. A. Crossley, and J. Fitch, "Design of dependable and secure system integrity protection schemes," *Int. J. Electr. Power Energy Syst.*, vol. 68, pp. 15–25, Jun. 2015, doi: 10.1016/j.ijepes.2014.12.047.
[14] G. Feng and A. Abur, "Fault location using wide-area measurements and sparse estimation," *IEEE Trans. Power Syst.*, vol. 31, no. 4, pp. 2938–2945, Jul. 2016, doi: 10.1109/TPWRS.2015.2469606.
[15] P. Kundu and A. K. Pradhan, "Enhanced protection security using the system integrity protection scheme (SIPS)," *IEEE Trans. Power Del.*, vol. 31, no. 1, pp. 228–235, Feb. 2016, doi: 10.1109/TPWRD.2015.2459231.
[16] A. G. Phadke, P. Wall, L. Ding, and V. Terzija, "Improving the performance of power system protection using wide area monitoring systems," *J. Mod. Power Syst. Clean Energy*, vol. 4, no. 3, pp. 319–331, Jul. 2016, doi: 10.1007/s40565-016-0211-x.
[17] A. Xue, F. Xu, K. E. Martin, H. You, J. Xu, L. Wang, and G. Wei, "Robust identification method for transmission line parameters that considers PMU phase angle error," *IEEE Access*, vol. 8, pp. 86962–86971, 2020, doi: 10.1109/ACCESS.2020.2992247.
[18] D.-I. Kim, T. Y. Chun, S.-H. Yoon, G. Lee, and Y.-J. Shin, "Wavelet-based event detection method using PMU data," *IEEE Trans. Smart Grid*, vol. 8, no. 3, pp. 1154–1162, May 2017, doi: 10.1109/TSG.2015.2478421.
[19] N. Liu and P. Crossley, "Assessing the risk of implementing system integrity protection schemes in a power system with significant wind integration," *IEEE Trans. Power Del.*, vol. 33, no. 2, pp. 810–820, Apr. 2018, doi: 10.1109/TPWRD.2017.2759181.
[20] S. M. Hashemi, M. Sanaye-Pasand, and M. Shahidehpour, "Fault detection during power swings using the properties of fundamental frequency phasors," *IEEE Trans. Smart Grid*, vol. 10, no. 2, pp. 1385–1394, Mar. 2019, doi: 10.1109/TSG.2017.2765200.
[21] D. S. Kumar and J. S. Savier, "Synchrophasor-based system integrity protection scheme for an ultra-mega-power project in India," *IET Gener., Transmiss. Distrib.*, vol. 13, no. 8, pp. 1220–1228, Apr. 2019, doi: 10.1049/iet-gtd.2018.5510.
[22] P. Gawande and S. Dambhare, "New predictive analytic-aided response-based system integrity protection scheme," *IET Gener., Transmiss. Distrib.*, vol. 13, no. 8, pp. 1204–1211, Apr. 2019, doi: 10.1049/iet-gtd.2018.5585.
[23] S. V. Unde, P. Gawande, and S. Dambhare, "New algorithm for protection of double circuit transmission lines using modal currents," *IEEE Trans. Power Del.*, vol. 34, no. 5, pp. 1967–1977, Oct. 2019, doi: 10.1109/TPWRD.2019.2906939.
[24] K. G. Ravikumar and A. K. Srivastava, "Designing centralised and distributed system integrity protection schemes for enhanced electric grid resiliency," *IET Gener., Transmiss. Distrib.*, vol. 13, no. 8, pp. 1194–1203, Apr. 2019, doi: 10.1049/iet-gtd.2018.5381.
[25] P. Gawande and S. Dambhare, "Pilot scheme for system integrity protection during stressed conditions," in *Proc. 8th Int. Conf. Power Syst. (ICPS)*, Jaipur, India, 2019, pp. 1–4, doi: 10.1109./ ICPS 48983.2019.9067634.
[26] S. Skok and I. Ivankovic, "System integrity protection schemes for future power transmission system using synchrophasors," *Int. Conf. Smart Grid Synchronized Meas. Analytics (SGSMA)*, College Station, TX, USA, 2019, pp. 1–7, doi: 10.1109./ SGSMA 2019.8784463.
[27] Zbunjak and Kuzle, "System integrity protection scheme (SIPS) development and an optimal bus-splitting scheme supported by phasor measurement units (PMUs)," *Energies*, vol. 12, no. 17, p. 3404, Sep. 2019, doi: 10.3390/en12173404.
[28] M. Mehrabankhomartash, M. Saeedifard, and S. Grijalva, "Model predictive control based AC line overload alleviation by using multi-terminal DC grids," *IEEE Trans. Power Syst.*, vol. 35, no. 1, pp. 177–187, Jan. 2020, doi: 10.1109/TPWRS.2019.2927548.
[29] B. Mallikarjuna and J. B. R. Maddikara, "Synchrophasor measurement-assisted system integrity protection scheme for smart power grid," *J. Control, Autom. Electr. Syst.*, vol. 31, no. 1, pp. 207–225, Feb. 2020.

[30] P. Wang and M. Govindarasu, "Multi-agent based attack-resilient system integrity protection for smart grid," *IEEE Trans. Smart Grid*, vol. 11, no. 4, pp. 3447–3456, Jul. 2020, doi: 10.1109/TSG.2020.2970755.
[31] K. B. Swain, S. S. Mahato, and M. Cherukuri, "Expeditious situational awareness-based transmission line fault classification and prediction using synchronized phasor measurements," *IEEE Access*, vol. 7, pp. 168187–168200, 2019, doi: 10.1109/ACCESS.2019.2954337.
[32] J. Kim, H.-T. Kim, and S. Choi, "Performance criterion of phasor measurement units for distribution system state estimation," *IEEE Access*, vol. 7, pp. 106372–106384, 2019, doi: 10.1109/ACCESS.2019.2932940.
[33] S. M. Blair, M. H. Syed, A. J. Roscoe, G. M. Burt, and J.-P. Braun, "Measurement and analysis of PMU reporting latency for smart grid protection and control applications," *IEEE Access*, vol. 7, pp. 48689–48698, 2019, doi: 10.1109/ACCESS.2019.2903929.
[34] *Central Electricity Regulatory Commission*. Accessed: Nov. 5, 2020. [Online]. Available: http//www.cercind.gov.in/
[35] *Western Regional Power Committee*. Accessed: Nov. 8, 2020. [Online]. Available: http//www.wrpc.gov.in/
[36] H. You, V. Vittal, and X. Wang, "Slow coherency-based islanding," *IEEE Trans. Power Syst.*, vol. 19, no. 1, pp. 483–491, Feb. 2004, doi: 10.1109/TPWRS.2003.818729.
[37] *E-Tap 7.0.0 Demo Guide by Operation*. Accessed: Aug. 10, 2020. [Online]. Available: http://docshare04.docshare.tips/files/

MAKARAND SUDHAKAR BALLAL (Senior Member, IEEE) received the B.E. degree in electrical engineering from the Government College of Engineering, Aurangabad, India, in 1993, the M.Tech. degree in integrated power system from the Visvesvaraya National Institute of Technology, Nagpur, India, in 1997, and the Ph.D. degree from Rashtrasant Tukadoji Maharaj Nagpur University, Nagpur, in 2007. From 1997 to 2012, he was with Maharashtra State Electricity Transmission Company Ltd., Mumbai, India, where he worked on the commissioning, installation, testing, and maintenance of various HV and EHV electrical equipment and accessories. He has 15 years of experience in the power sector. He is currently working as a Professor with the Department of Electrical Engineering, Visvesvaraya National Institute of Technology. His research interests include condition monitoring of electrical machines, power quality measurements, and power electronics and drives.

AMIT RAMCHANDRA KULKARNI (Student Member, IEEE) received the master's degree in electrical power systems from the University of Pune, in 2005. He has worked on project in system studies with the Indian Institute of Technology Bombay, India. He is currently as an Additional Executive Engineer working with Maharashtra State Electricity Transmission Company Ltd. He has worked in various areas like power system studies and regulatory affairs, protection, testing and transmission project execution, smart grid, and automation project development. He was instrumental in implementing India's first Wide Area Measurement System (WAMS) project grid wise in the state of Maharashtra in India. He is a part of various State and Regional level study Groups in India working in above areas. His research interests include power system stability, power system planning and studies, power system operation, control and grid management, power system protection, and smartgrid areas like WAMS, FACTS, and renewable energy management systems (REMS).